

A mechanistic population balance model to evaluate the impact of interventions on infectious disease outbreaks: Case for COVID19

Jorge Rodríguez^{1*}, Juan M Acuña², Joao M Uratani¹ and Mauricio Patón¹

¹Department of Chemical Engineering. College of Engineering. Khalifa University. SAN Campus PO Box 2533 Abu Dhabi, United Arab Emirates

²Department of Epidemiology and Public Health. College of Medicine. Khalifa University. PO Box 127788 Abu Dhabi, United Arab Emirates

*Corresponding author: jorge.rodriguez@ku.ac.ae

Abstract

Infectious diseases, especially when new and highly contagious, could be devastating producing epidemic outbreaks and pandemics. Predicting the outcomes of such events in relation to possible interventions is crucial for societal and healthcare planning and forecasting of resource needs. Deterministic and mechanistic models can capture the main known phenomena of epidemics while also allowing for a meaningful interpretation of results. In this work a deterministic mechanistic population balance model was developed. The model describes individuals in a population by infection stage and age group. The population is treated as in a close well mixed community with no migrations. Infection rates and clinical and epidemiological information govern the transitions between stages of the disease. The present model provides a steppingstone to build upon and its current low complexity retains accessibility to non experts and policy makers to comprehend the variables and phenomena at play.

The impact of specific interventions on the outbreak time course, number of cases and outcome of fatalities were evaluated including that of available critical care. Data available from the COVID19 outbreak as of early April 2020 was used. Key findings in our results indicate that (i) universal social isolation measures appear effective in reducing total fatalities only if they are strict and the number of daily social interactions is reduced to very low numbers; (ii) selective isolation of only the elderly (at higher fatality risk) appears almost as effective in reducing total fatalities but at a much lower economic damage; (iii) an increase in the number of critical care beds could save up to eight lives per extra bed in a million population with the current parameters used; (iv) the use of protective equipment (PPE) appears effective to dramatically reduce total fatalities when implemented extensively and in a high degree; (v) infection recognition through random testing of the population, accompanied by subsequent (self) isolation of infected aware individuals, can dramatically reduce the total fatalities but only if conducted extensively to almost the entire population and sustained over time; (vi) ending isolation measures while R_0 values remain above 1.0 (with a safety factor) renders the isolation measures useless and total fatality numbers return to values as if nothing was ever done; (vii) ending the isolation measures for only the population under 60 y/o at R_0 values still above 1.0 increases total fatalities but only around half as much as if isolation ends for everyone; (viii) a threshold value, equivalent to that for R_0 , appears to exist for the daily fatality rate at which to end isolation measures, this is significant as the fatality rate is (unlike R_0) very accurately known.

Any interpretation of these results for the COVID19 outbreak predictions and interventions should be considered only qualitatively at this stage due to the low confidence (lack of complete and valid data) on the parameter values available at the time of writing. Any quantitative interpretation of the results must be accompanied with a critical discussion in terms of the model limitations and its frame of application.

Introduction

Understanding the potential spread of diseases using mathematical modelling approaches has a long history. Deterministic epidemic models published in the early 20th century already demonstrated the importance of understanding the population-based dynamics as well as potential parameters of interest therein (Kermack & McKendrick, 1927). Numerous modelling approaches are available for the prediction of propagation of infectious diseases (May & Anderson, 1979; Capasso & Wilson, 1997; Hethcote, 2000; McCallum *et al.*, 2001; Ruan & Wang, 2003; Li *et al.*, 2004; Keeling & Eames, 2005; Grassly & Fraser, 2008; Keeling & Rohani, 2008; Balcan *et al.*, 2010; Britton, 2010; Funk *et al.*, 2010; Gray *et al.*, 2011; Brauer *et al.*, 2012; Miller *et al.*, 2012; Siettos & Russo, 2013; Pastor-Satorras *et al.*, 2015). Their outputs inform studies on health projections and play an important role in shaping policies related to public health (Murray and Lopez, 1997a, 1997b, 1997c, and 1997d; Ferguson *et al.*, 2006).

Data availability has greatly increased in recent years, which led to direct improvements in epidemiological models (Colizza *et al.*, 2006; Riley, 2007; Siettos & Russo, 2013). These models provided a more comprehensive understanding of recent outbreaks of diseases such as Ebola (Gomes *et al.*, 2014; WHO Ebola Response Team, 2014) and Zika (Zhang *et al.*, 2017). However, all modelling efforts are highly dependent on several elements: a comprehensive algorithm of clinical and public health true options and stages of events; probability of such options given certain conditions of the system; identification of parameters that reflect such events and their probabilities (such as mortality by age, infectiousness by contacts, etc.); assumptions for parameters with insufficient data; and valid data for those parameters that allow the calibration and posterior validation of the forecasts (Tizzoni *et al.*, 2012).

In viral pandemics in particular, one of those parameters, the direct estimation of infected sub-population fractions, is not feasible using available epidemiological data (unless universal, highly sensitive testing is used, rarely possible to implement in these situations), particularly if very mild cases, asymptomatic infections or pre-symptomatic transmission are observed or expected. This was the case of the previous Influenza A (H1N1-2009) pandemic (Nishiura *et al.*, 2011) and it is the observation for COVID-19 pandemic (Russel *et al.*, 2020). Thus, in many cases, modelling uses a combination of the best available data from historical events and datasets, parameter estimation and assumptions. Then, data about these parameters are computed with statistical tools for the development of epidemic models (Cooper *et al.*, 2006; Biggerstaff *et al.*, 2014).

The most challenging phase for the understanding of the potential spread of a disease is when novel disease outbreaks emerge in global populations (Anderson & May, 1992), in which data availability is limited (e.g. novelty of pathogen; delay of communication of case datasets from public health workers and facilities to researchers) or biased by external factors (e.g., limited availability of testing capacity; undefined or partially defined diagnostics for disease). With novel disease-specific epidemic models, the development of models with the sufficient level of low complexity and meaningful parameters, that can be identified with data as the infection progresses and data become more available, is posited as a potential tool to inform public health policy and impact mitigation strategies (Berezovskaya *et al.*, 2005; Hall *et al.*, 2007; Bettencourt *et al.*, 2008; Nishiura, 2011; Wang & Zhao, 2012; Lee *et al.*, 2013; Nsoesie *et al.*, 2014; Chowell *et al.*, 2016; Rivers *et al.*, 2019; Chowell *et al.*, 2020). The parameters of these models can be identified with data as the infection progresses and data become more available.

The COVID-19 outbreak and posterior pandemic has brought unprecedented attention into these kinds of modelling approach limitations, with multiple epidemic models and disease spread forecasts being published as more data becomes available. These models have evaluated the ongoing course of the disease spread evolution, from the earlier dynamics of transmission from

initial cases (Kucharski *et al.*, 2020), to the potential of non-pharmaceutical interventions to limit the disease spread, such as: international travel restrictions (Chinazzi *et al.*, 2020), contact tracing and isolation of infected individuals at onset (Hellewell *et al.*, 2020), different scales of social distancing and isolation (Flaxman *et al.*, 2020, Prem *et al.*, 2020). Other statistical models tried to estimate fundamental characteristics (*i.e.* potential model parameters) for the disease, such as the incubation period (Lauer *et al.*, 2020) and basic reproduction number, R_0 (Liu *et al.*, 2020), as well as to assess short-term forecasts (Roosa *et al.*, 2020). Given the inherent uncertainty associated with most of the parameters used, a stochastic approach is employed in the above models.

Effective communication between health care and public health systems and science hubs is considered one of the bigger challenges in both health sciences and public health (Zarcadoolas, 2010; Squiers *et al.*, 2012). In health care It is not only necessary to take effective measures but also to do it timely. This requires strategies for data sharing, generation of information and knowledge and timely dissemination of such knowledge for effective implementations.

The development of strategies for interaction under the general, and correct assumption of low literacy health communication paradigms are especially relevant (Plimpton & Root, 1994). And we have good evidence that health illiteracy influences greatly health behaviours that in turn, are likely to play a role in influencing the degree of the effectiveness of such interventions. Given the complexity and the expected short and long-lasting impacts that these public health interventions should have when dealing with disease outbreaks and pandemics (Reluga, 2010; Fenichel *et al.*, 2011) sufficiently complex but user-accessible modelling tools should provide researchers, public health authorities, and the general public with useful information to act in moments of clear and wide uncertainty. In order to work properly they require access to up-to-date data, in this case of the COVID-19 spread (Dong *et al.*, 2020). Additionally, simple and interactive models can contribute to the understanding by broader audiences of what to expect on the propagation of infectious diseases and how specific interventions may help. This increased awareness of the disease behaviour and potential course in time by public and policy makers can directly and positively impact the outcome of epidemic outbreaks (Funk *et al.*, 2009).

Population balance models are widely use in disciplines such as chemical engineering to describe the evolution of a population of particles (Henze *et al.*, 2000; Ramkrishna and Singh, 2014; Yang, 2014; González-Peñas *et al.*, 2020). These types of models describe the variation over time of, so-called, state variables as functions of state transition equations governed by transport processes, chemical reactions or any type of change rate from one state to another. Such models allow for the description of the underlying processes in a mechanistic manner, maintaining therefore a direct interpretation of the model behaviour. If the state transition rates are defined in mechanistic manner and with meaningful parameters, such models can describe a process in a way that is interpretable into reality and open the possibility not only of prediction but also of hypothesis generation when data deviate from model predictions.

The present work attempts to provide a deterministic population balance-based model with a sufficient minimum, but clinically and public health robust, set of mechanistic and interpretable parameters and variables. The model aims at improving the understanding of the major phenomena involved and of the impacts in the system's resources and needs of several possible interventions. The model level of complexity is targeted such that retains mechanistic meaning of all variables and parameters, captures the major phenomena at play and specifically allows for accessibility to non-experts and policy makers to comprehend the variables at play. I this way expert advice and decision making can be brought closer together to help guide interventions for immediate and longer-term needs.

Model description

The model presented is based on balances of individuals transitioning between infection stages and segregated by age group. All individuals are placed in a common single domain or close community (e.g. a well-mixed city or town), no geographical clustering nor separation of any type is considered, neither is any form of migration in or out of the community. Big cities with ample use of public transportation are thought to be settings best described by the model.

The model also provides a direct estimation of the R_0 (reproduction number or reproductive rate) (Delamater *et al.* 2019) under different circumstances of individual characteristics (such as personal protection or awareness) as well as under population-based interventions (such as imposed social isolation). R_0 is a dynamic number often quoted erroneously as a constant for a specific microorganism or disease. The ability to estimate the R_0 for different times of the outbreak (given the interventions), outbreak settings and interventions is considered to be a valuable model characteristic. R_0 is predicted to change over time with interventions that do not produce immune subjects (such as isolation or use of personal protection equipment (PPE), as opposed to vaccination). However, in many instances over the course of an outbreak, R_0 is consistently estimated as a constant, frequently overestimating and not allowing correct estimations of the course of events.

Model constituents

The model solves dynamic variables or states. Every individual belongs, in addition to their age group (which she/he never leaves), to only one of the possible states that correspond to stages of the infection, namely: *Healthy-non-susceptible* (HN); *healthy susceptible* (H); *pre-symptomatic* (PS); *symptomatic* (S); *hospitalised* (SH); *critical* (SC) (with and without available intensive care); *deceased* (D) and *recovered immune* (R).

Definitions of the model states are shown in Table 1. Each variable is a state vector with the number of individuals in that stage per age group. Age groups are defined per decade from 0-9 until 80+ year olds. Nine age groups are defined in the model, each state is therefore a vector of dimensions 1x9, the total number of states is a matrix of dimensions 8x9. The transitions between these states are governed by rates of infection and transition as defined in Table 2. Note that vector variables and parameters are represented in bold font and scalar ones in regular font.

Table 1. Model states in vectors (1x9) of number of individuals in each infection stage.

Definition "Number of..."	Variable	Totals of all ages
Healthy non-susceptible to infection	\mathbf{N}_{hn}	N_{hnT}
Healthy susceptible to infection	\mathbf{N}_h	N_{hT}
Pre-symptomatic infected	\mathbf{N}_{ps}	N_{psT}
Symptomatic infected	\mathbf{N}_s	N_{sT}
Symptomatic hospitalised	\mathbf{N}_{sh}	N_{shT}
Symptomatic critical	\mathbf{N}_{sc}	N_{scT}
Deceased	\mathbf{N}_d	N_{dT}
Recovered & immune	\mathbf{N}_r	N_{rT}

A schematic representation of the modelling approach with the population groups considered for the infection stages, rates of infection and transition between groups and showing possible interactions between population groups is shown in Figure 1.

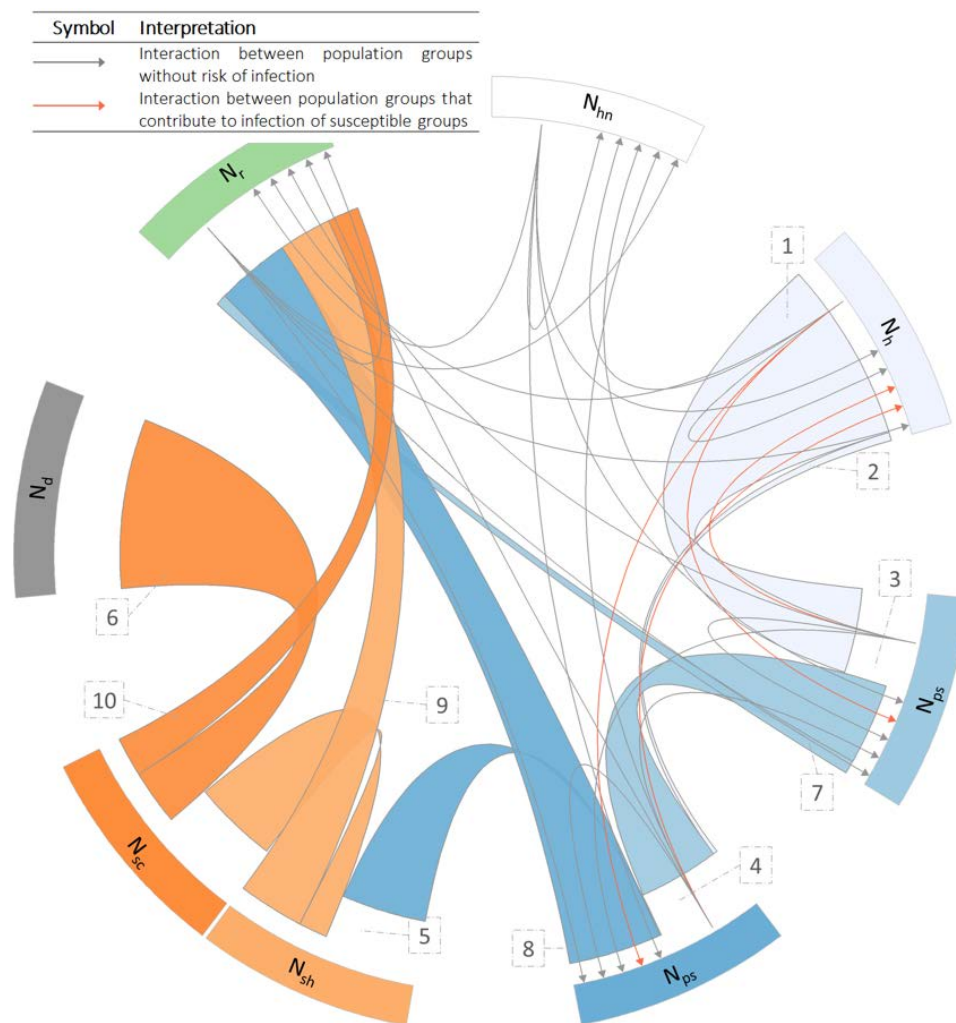


Figure 1. Schematic representation of the modelling approach showing the population groups considered to describe the infection stages. Each arc segment represents one of the model states, while the coloured bands represent the rate of infection and transition between groups. Band width is proportional to the average rates across population ages, demographically weighted for the scenario assessed. The arrows indicate the possible interactions between population groups that are part of the calculation of the rates of infection. Only interactions between infected individuals (both pre-symptomatic and symptomatic) and healthy susceptible ones can increase the rate of infections (red arrows).

Table 2. Rates of infection and transition between states, vectors (1x9).

Definition “Rate of ...”	Variable	Units
Infection by interaction with infected pre-symptomatic	r_{i_ps}	# H infected/day
Infection by interaction with infected symptomatic	r_{i_s}	# H infected/day
Transition to symptomatic from infected	r_{s_ps}	# PS to S / day
Transition to hospitalised from symptomatic	r_{sh_s}	# S to SH / day
Transition to critical from hospitalised	r_{sc_sh}	# SH to SC / day
Transition to deceased from critical	r_{d_sc}	# SC to D / day
Recovery from pre-symptomatic infected	r_{r_ps}	# PS to R / day
Recovery from symptomatic infected	r_{r_s}	# S to R / day
Recovery from hospitalised	r_{r_sh}	# SH to R / day
Recovery from critical	r_{r_sc}	# SC to R / day

Modelling interventions

Two main interventions are described in the model that have are being used currently slow the spread of the COVID19 disease outbreak (i) the *degree of social isolation* of the individuals in the population in terms of the average number of random interaction individuals have per day with others that are also interacting and (ii) the *level of personal protection and awareness* that individuals have to protect themselves and others against contagion or spread during interactions. These interventions can be stratified by age groups. Table 3 describes the key parameters that define the interventions.

The degree of isolation is described by a parameter (\mathbf{ni}_h) (vector per age group) corresponding to a representative average number of daily interactions that healthy susceptible individuals have with others. Different \mathbf{ni}_h values can be assigned per age group to describe the impact of diverse isolation strategies selective to age group such as e.g. selective isolation of the elderly and/or young. The level of use of PPE and awareness described by the parameters (\mathbf{lpa}_h) for healthy and (\mathbf{lpa}_{ps} and \mathbf{lpa}_s) for infectious individuals (both in vectors per age group). Values of the \mathbf{lpa} parameters can vary between 0 and 1, with 1 corresponding to the use of complete protective measures and zero to the most reckless opposite situation.

An additional reduction factor is defined for decreased social interactivity of infectious individuals both for symptomatic (\mathbf{rfi}_s), to describe e.g. self or imposed isolation of S individuals and for pre-symptomatic (\mathbf{rfi}_{ps}), to describe e.g. awareness of their infection if extensive random testing of the population is implemented.

Table 3. Intervention parameters

Definition	Parameter	Units
Average daily individual interactions by H	ni_h	#interactions / H individual·day
Reduction factor of daily interactions by S ¹	r_{fi_s}	∅
Reduction factor of daily interactions by PS ¹	$r_{fi_{ps}}$	∅
Level of personal protection and awareness by H ¹	lpa_h	∅
Level of personal protection and awareness by PS ¹	lpa_{ps}	∅
Level of personal protection and awareness by S ¹	lpa_s	∅
Probability of infection per interaction with PS ²	$p_{i_{ps}}$	infections / interactions with PS
Probability of infection per interaction with S ²	p_{i_s}	infections / interactions with S

¹Values only within the interval [0,1]; ²Calculated, not an input parameter.

Rates of infection

The infection of healthy susceptible individuals (H) is modelled as to occur only by interaction between them and other infected either pre-symptomatic (PS) or symptomatic (S) individuals. Infected hospitalised (SH) and critical (SC) are assumed not available for infectious interactions neither are those deceased (D).

Two rates of infection of healthy susceptible individuals (in number of infections per day) are defined, one from each one of the two possible infecting groups (PS and S). The rates of infection are vectors per age group from the product of (i) the fraction of interactions with PS (or S) among the total interactions (f_{ips} or f_{is}) times (ii) the probability of contagion in an interaction with PS (or S) ($p_{i_{ps}}$ or p_{i_s}) (per age group), (iii) the average number of daily interactions that H individuals have (ni_h) and (iv) the number of H individuals themselves (per age group) (see Eqs 1.a-b). Note that point operators between vectors indicate an operation element-by-element.

$$r_{i_{ps}} = f_{ips} * (p_{i_{ps}} * ni_h * N_h); \quad (\text{Eq. 1.a})$$

$$r_{i_s} = f_{is} * (p_{i_s} * ni_h * N_h); \quad (\text{Eq. 1.b})$$

The fractions of interactions (f_{ips} and f_{is}) among the total are calculated as per Eqs 2.a-b. Note that hospitalised, critical and deceased are excluded from the pool of possible interacting individuals.

$$f_{ips} = \sum (r_{fi_{ps}} * N_{ps}) / \sum [N_{hn} + N_h + (r_{fi_{ps}} * N_{ps}) + (r_{fi_s} * N_s) + N_r] \quad (\text{Eq. 2.a})$$

$$f_{is} = \sum (r_{fi_s} * N_s) / \sum [N_{hn} + N_h + (r_{fi_{ps}} * N_{ps}) + (r_{fi_s} * N_s) + N_r] \quad (\text{Eq. 2.b})$$

The probabilities of infection per interaction are calculated as per Eq. 2.c-d..

$$p_{i_{ps}} = (1 - lpa_h) * (1 - lpa_{ps}^{av}); \quad (\text{Eq. 2.c})$$

$$p_{i_s} = (1 - lpa_h) * (1 - lpa_s^{av}); \quad (\text{Eq. 2.d})$$

where lpa_{ps}^{av} and lpa_s^{av} are scalars corresponding to the weighted averages (Eqs 2.e-f) over age groups of the entire pool of PS and S with which H individuals can interact. N_{asT} and N_{sT} are the total numbers of PS and S individuals of all ages respectively. The \sum symbol indicates summation across all age groups.

$$lpa_{ps}^{av} = \sum (N_{as} * lpa_{ps}) / N_{asT} \quad (\text{Eq. 2.e})$$

$$lpa_s^{av} = \sum (N_s * lpa_s) / N_{sT} \quad (\text{Eq. 2.f})$$

Rates of transition between infection stages

The average rates of transition between states are defined such that epidemiological and clinical available data can be used such as the proportion of individuals that transition or recover (see Table 4) and the average times reported at each stage before transition or recovery (see Table 5).

Table 4. Epidemiological parameters (all in vectors per age group).

Definition	Parameter	Units	
Fraction of population non-susceptible to infection	f_{hn_t}	#HS/#H	
Fraction of PS that will become S ¹	$(1 - f_{r_{ps}})$	$f_{s_{ps}}$	#S/#PS
Fraction of S that will become SH	$(1 - f_{r_{ss}})$	f_{sh_s}	#SH/#S
Fraction of SH that will become SC	$(1 - f_{r_{sh}})$	$f_{sc_{sh}}$	#SC/#SH
Fraction of cared SC that will die into D	$(1 - f_{r_{sc}})$	$f_{d_{sc}}$	#D/#SC _{IC}
Fraction of PS that will recover into R		$f_{r_{ps}}$	#R/#PS
Fraction of S that will recover into R		f_{r_s}	#R/#S
Fraction of SH that will recover into R		$f_{r_{sh}}$	#R/#SH
Fraction of SC with critical care that will recover into R		$f_{r_{sc}}$	#R/#SC _{IC}

¹Calculated, not an input parameter

Table 5. Clinical average times in each infection stage (all in vectors per age group).

Definition	Parameter	Units
Time to develop symptoms (incubation period)	$t_{s_{ps}}$	days
Time to become hospitalised if symptomatic	t_{sh_s}	days
Time to become critical if hospitalised	$t_{sc_{sh}}$	days
Time to death from critical	$t_{d_{sc}}$	days
Time to death from critical with no IC available	$t_{d_{nc}}$	days
Time to recover without symptoms	$t_{r_{ps}}$	days
Time to recover from (non-severe) symptoms	t_{r_s}	days
Time to recover from hospitalisation	$t_{r_{sh}}$	days
Time to recover from critical	$t_{r_{sc}}$	days

The rates of individuals transitioning between stages (in number of individuals per day) are described in Eqs 3.a-e. All rates are vectors per age group of dimensions (1x9).

$$r_{ps_h} = r_{i_{ps}} + r_{i_s} \quad (\text{Eq. 3.a})$$

$$r_{s_{ps}} = f_{s_{ps}} \cdot N_{ps} / t_{s_{ps}} \quad (\text{Eq. 3.b})$$

$$r_{sh_s} = f_{sh_s} \cdot N_s / t_{sh_s} \quad (\text{Eq. 3.c})$$

$$r_{sc_{sh}} = f_{sc_{sh}} \cdot N_{sh} / t_{sc_{sh}} \quad (\text{Eq. 3.d})$$

In order to describe the possible shortage of critical care resources, critical individuals are distributed between those with available intensive care ($N_{sc_{ic}}$) and those without available intensive care ($N_{sc_{nc}}$). At each simulation time step $N_{sc_{ic}}$ and $N_{sc_{nc}}$ are computed via an allocation function of critical care resources over the total N_{sc} per age group. The function allocates resources with priority to lower age groups until the maximum number of intensive care units is reached. All critical

individuals with no available intensive care N_{sc_nc} are assumed to become deceased after t_{d_nc} . The rate of transition from critical to deceased is therefore the sum of that of those with available care (r_{d_scic}) plus that of those without available care (r_{d_scnc}) as per Eqs. 3.e-g.

$$r_{d_sc} = r_{d_scic} + r_{d_scnc} \quad (\text{Eq. 3.e})$$

where

$$r_{d_scic} = f_{d_sc} \cdot N_{sc_ic} / t_{d_sc} \quad (\text{Eq. 3.f})$$

$$r_{d_scnc} = N_{sc_nc} / t_{d_nc} \quad (\text{Eq. 3.g})$$

The rates of individuals recovering from the different infected stages (in number of individuals per day) are described in Eqs 4.a-d. (all rates in vectors per age group).

$$r_{r_ps} = f_{r_ps} \cdot N_{ps} / t_{r_ps} \quad (\text{Eq. 4.a})$$

$$r_{r_s} = f_{r_s} \cdot N_s / t_{r_s} \quad (\text{Eq. 4.b})$$

$$r_{r_sh} = f_{r_sh} \cdot N_{sh} / t_{r_sh} \quad (\text{Eq. 4.c})$$

$$r_{r_sc} = f_{r_sc} \cdot N_{sc_ic} / t_{r_sc} \quad (\text{Eq. 4.d})$$

Stage transition equations

The dynamic variation on the number of individuals in each stage over time and per age groups is governed by the population balance equations described in Eqs 5.a-h. (all in vectors by age group).

$$dN_{hn}/dt = 0; \quad (\text{Eq. 5.a})$$

$$dN_h/dt = -r_{ps_h} \quad (\text{Eq. 5.b})$$

$$dN_{ps}/dt = r_{ps_h} - r_{s_ps} - r_{r_ps} \quad (\text{Eq. 5.c})$$

$$dN_s/dt = r_{s_ps} - r_{sh_s} - r_{r_s} \quad (\text{Eq. 5.d})$$

$$dN_{sh}/dt = r_{sh_s} - r_{sc_sh} - r_{r_sh} \quad (\text{Eq. 5.e})$$

$$dN_{sc}/dt = r_{sc_sh} - r_{d_sc} - r_{r_sc} \quad (\text{Eq. 5.f})$$

$$dN_d/dt = r_{d_sc} \quad (\text{Eq. 5.g})$$

$$dN_r/dt = r_{r_ps} + r_{r_s} + r_{r_sh} + r_{r_sc} \quad (\text{Eq. 5.h})$$

The state transitions as governed by these rates are represented in a matrix form in Figure A2.

Reproduction number (R_0) and its calculation

Since the model produces instant values of outputs over time based on the parameters used, the reproduction number (R_0) simulated must be considered as an instantaneous estimation of the R_0 (Delamater *et al.* 2019). The model structure allows for several parameters to influence R_0 including the duration of infectious stages for the virus known so far; the potential infection of others by the virus from those infected; the probabilities of infection per social interaction; and other parameters such social isolation and use of PPE. Elements such as the number of recovered immune individuals should not directly affect R_0 as the reproductive number refers to only the potential infection of susceptible individuals from infected individuals.

Dynamic reproduction number (R_0) during the outbreak (Delamater *et al.* 2019) is computed over time from the model state variables according to Eq. 6. Under this approach, infectious individuals can only infect others while they are in pre-symptomatic (PS) and symptomatic (S) stages. Although it is known that post-symptomatic recovered individuals may be infectious for some period of time, this has not been considered in the model at this time due to lack of data. Hospitalised and critical

individuals are assumed to be well isolated and also not able to infect others. The provided dynamic output of the reproduction number R_0 can be used to guide and interpret the impact of interventions in terms of R_0 .

Modelled infected individuals can take only three possible infectious paths namely: (i) $PS \rightarrow R$; (ii) $PS \rightarrow S \rightarrow R$ and (iii) $PS \rightarrow S \rightarrow SH$. These paths are made of combinations of four possible infectious stage intervals in which infected individuals spend time and infect at their corresponding rate (see Table 6).

Table 6. Possible infectious stages intervals for R_0 computation.

Infectious interval	Fraction of infected passing the interval (ind_{interv}/ind_{inf})	Interval duration (d)	Total infections per stage interval per individual infected (inf_{interv}/ind_{inf})
$PS \rightarrow R$	$f_{r_{ps}}$	$t_{r_{ps}}$	$(r_{i_{psT}} / N_{psT}) * t_{r_{ps}} * f_{r_{ps}}$
$PS \rightarrow S$	$(1 - f_{r_{ps}})$	$t_{s_{ps}}$	$(r_{i_{psT}} / N_{psT}) * t_{s_{ps}} * (1 - f_{r_{ps}})$
$S \rightarrow R$	$(1 - f_{r_{ps}}) * f_{r_{s}}$	$t_{r_{s}}$	$(r_{i_{sT}} / N_{sT}) * t_{r_{s}} * (1 - f_{r_{ps}}) * f_{r_{s}}$
$S \rightarrow SH$	$(1 - f_{r_{ps}}) * (1 - f_{r_{s}})$	$t_{sh_{s}}$	$(r_{i_{sT}} / N_{sT}) * t_{sh_{s}} * (1 - f_{r_{ps}}) * (1 - f_{r_{s}})$

The dynamic computation of R_0 consists of adding the total infection contributions of every stage interval as shown in Eq. 7.

$$R_0 = \sum [(r_{i_{psT}} / N_{psT}) * (t_{r_{ps}} * f_{r_{ps}} + t_{s_{ps}} * (1 - f_{r_{ps}})) + (r_{i_{sT}} / N_{sT}) * (t_{r_{s}} * (1 - f_{r_{ps}}) * f_{r_{s}} + t_{sh_{s}} * (1 - f_{r_{ps}}) * (1 - f_{r_{s}}))] \quad (\text{Eq. 6})$$

in which, the age group weighted average rates of infection by PS and S are given as per Eqs. 6a-b.

$$r_{i_{psT}} = \sum (r_{i_{ps}} * N_{ps}) / N_{psT} \quad [inf_{ps}/ind_{ps} \cdot d] \quad (\text{Eq. 7.a})$$

$$r_{i_{sT}} = \sum (r_{i_{s}} * N_s) / N_{sT} \quad [inf_{ps}/ind_{ps} \cdot d] \quad (\text{Eq. 7.b})$$

Model limitations

The model presented is deterministic and based on population balances of individuals classified by their stage of infection and age group only, no other differentiation within those groups is captured by this version of the model. This characteristic allows for the model application to single, densely populated clusters. The model has low complexity and requires a small number of mechanistic meaningful parameters, most of which can be directly estimated from epidemiological and clinical data. The model however carries limitations in its prediction capabilities due to the fact that all variables and parameters refer to representative averages for each stage and age group population. This may limit the model representation of the non-linear interactions in the real system and therefore at this stage any results interpretation for prediction purposes should be critically discussed against these limitations.

Impact of static interventions on a COVID19 outbreak case study

A case study based on a scenario of propagation of the COVID19 pandemic using data available as of April 2020 is presented below. The results obtained are intended to be interpreted qualitatively and to be contextualized to the specific setting characteristics. They intend to serve as a demonstration of the model potential if applied with higher confidence parameter values. A number of selected scenarios aimed at illustrating the impact of different interventions were simulated. Conclusions should be taken qualitatively at this stage given the low confidence in some parameter values.

Default reference epidemiological and clinical parameter values were obtained from different information sources on the COVID19 outbreak as available in early April 2020. Details of values and sources are provided in the Appendix Tables A1-A2 respectively, with indication of level of confidence. A population with an age distribution as that of the region of Madrid (Spain) in 2019 was used (INE Spain, 2020).

Default reference intervention parameters were selected arbitrarily for a situation assimilated to that previous to the outbreak and without any specific intervention (see values and rationale in Appendix Table A3). The dynamic simulation results of the default outbreak scenario with no intervention is shown in in the Appendix Figure A4.

All scenarios are simulated for 365 days and evaluated in terms of (i) final total number of fatalities at outbreak termination and (ii) final number of fatalities per age group. In addition, the scenarios are presented also in terms of dynamic profiles over time for (iii) number of active cases; (iv) reproduction number; (iv) number of critical cases; (v) number of fatalities.

Scenario #1. Universal social isolation

In this scenario, the impact of different imposed degrees of universal social isolation was evaluated. The parameter that describes this intervention is the average number of daily social interactions that healthy susceptible individuals have (ni_h). As indicated above, evidence suggests that during viral infections that behave such as COVID-19, the number of personal contacts increases the likelihood of infection linearly. In this scenario, the isolation measures are applied equally across all age groups and the same ni_h values applied to all. Figure 2 illustrates the model predictions for this scenario, in terms of the output variables indicated and in absence of any other interventions.

As it can be observed in Figure 2 (top left), the overall risk of dying from the virus increases as the average number of daily social interactions (ni_h) increases. However, it seems to plateau at around 4 interactions per day, suggesting that a specific a critical value may exist for ni_h for the intervention to succeed at lowering the final number of deaths. Once age is placed in the equation, mortality behaves similarly only for those at ages over 70 (Figure 2 (top right)).

Interestingly, the ni_h does not appear to significantly modify mortality beyond a single interaction per day. This suggests that for younger than 60, interactions, in order to decrease mortality should be lower to 0: complete social distancing and isolation and that based only on social interactions, most of the mortality decreased by partial social isolation will be in those older than 60 years of age. The number of fatalities appears clearly and directly related to social isolation as well as the speed at which the fatalities saturation will occur, Figure 2(bottom right). The model is capable to capture this due to its description of the saturation of the healthcare capacity and withdrawal of critical care over capacity.

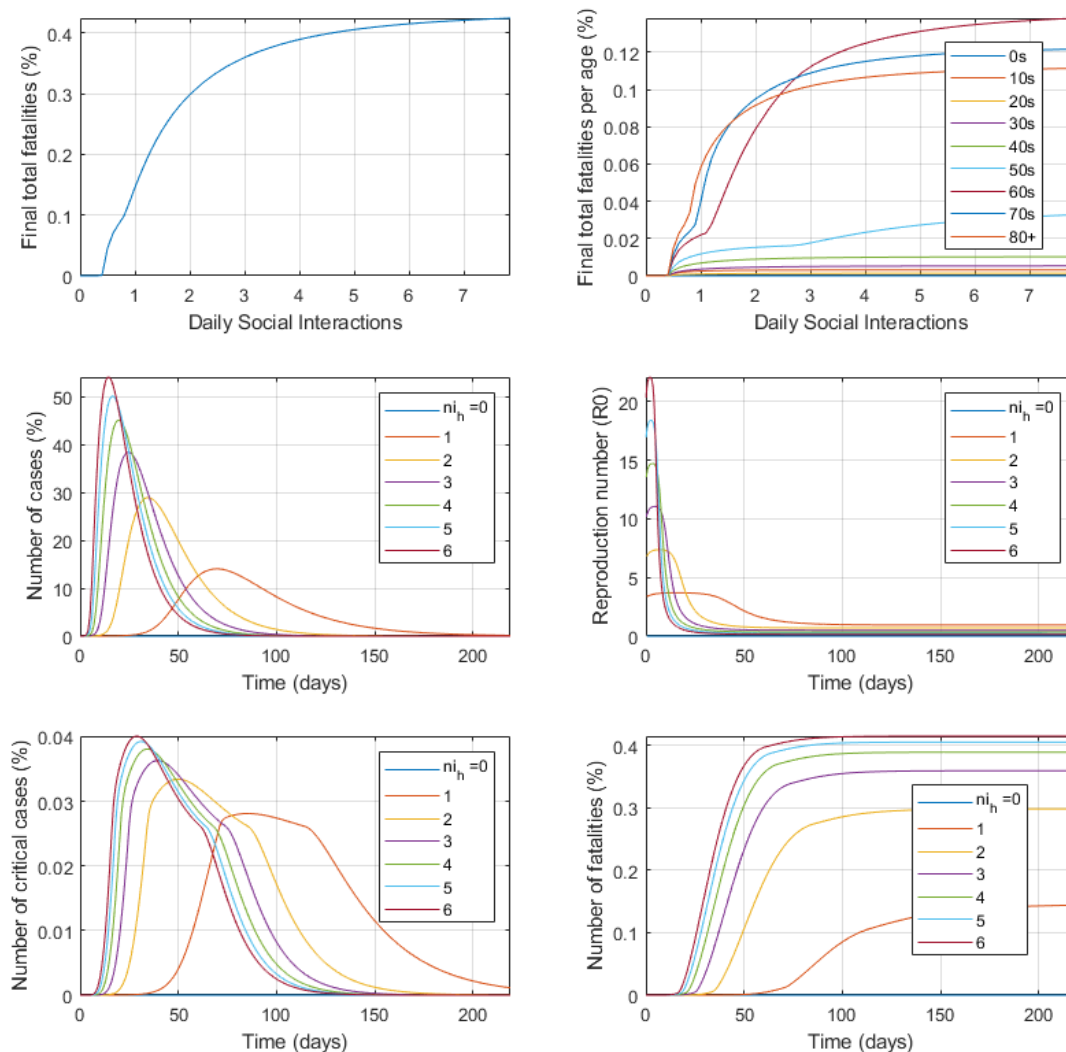


Figure 2. Impact of universal social isolation on the final total number of fatalities (top left); the final total number of fatalities per age group (top right) as well as for the different time course profiles of the total active cases (middle left); reproduction number (R_0) (middle right); the number of critical cases (bottom left) and the number of fatalities (bottom right). Numbers are as percentage of total population of all ages.

The middle and bottom graphs in Figure 2 show the impact of n_{i_h} on the time course of several variables. Figure 2(middle left) supports the “flatten the curve” concept, now globally popular. If interactions are not modified, the number of cases grows rapidly, exponentially and explosively. Figure 2(middle right) shows the estimate of R_0 over time. This illustrates how the levels of social isolation can define the infectability and the number of cases each infected individual will infect (R_0) showing how factors such as interventions can impact R_0 . The number of critical cases increases throughout time as the social interaction increases Figure 2(bottom left). However, with very low

Scenario #2. Selective social isolation of the elderly

The impact of imposed social isolation selective to those over 60 years old is evaluated in this scenario. The parameter that describes this intervention is the average number of daily social interactions with other people that healthy susceptible individuals within the age groups over 60 years old have (ni_h). In this scenario, the isolation measures are applied selectively only to the elderly. Figure 3 illustrates the model predictions for this scenario, in terms of the output variables indicated, in absence of any other interventions.

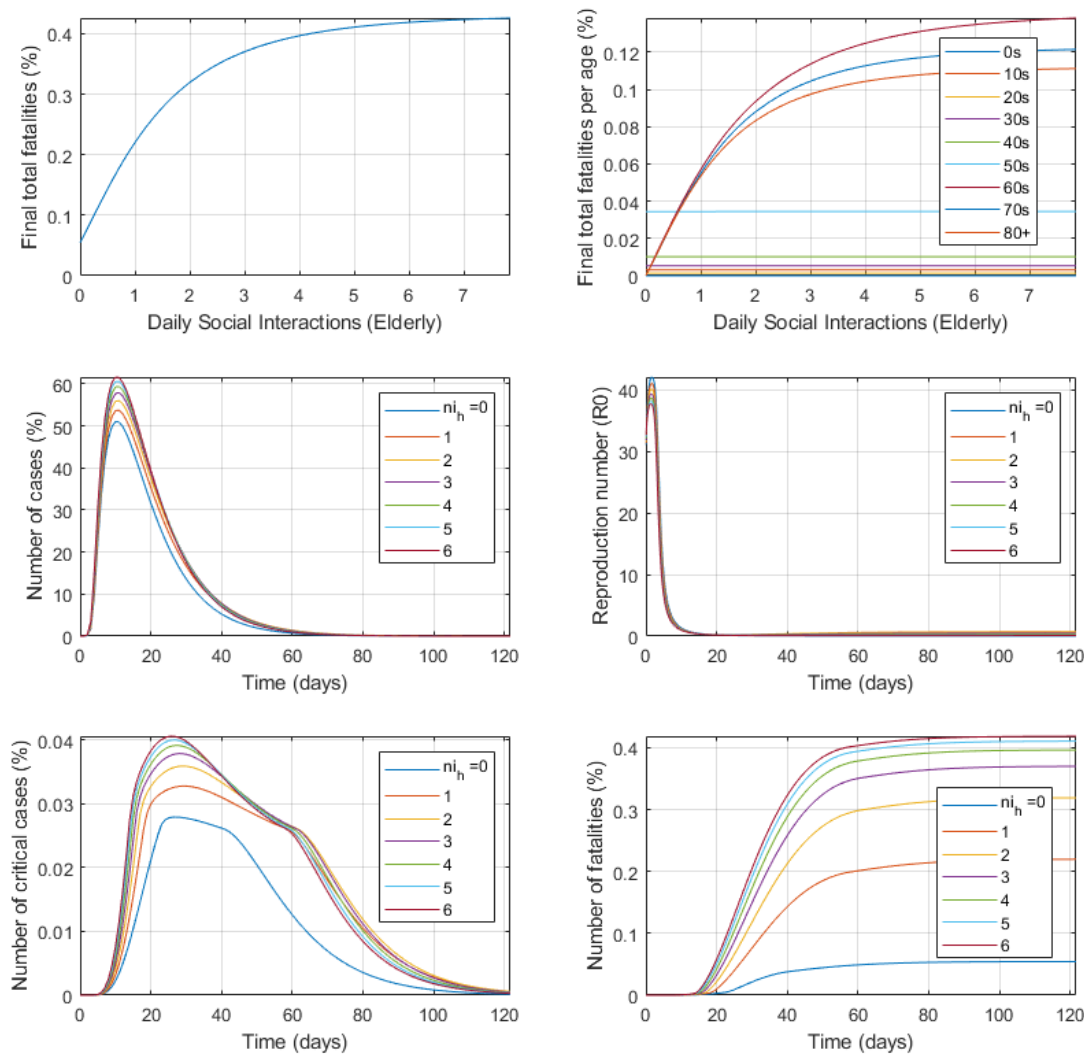


Figure 3. Impact of selective social isolation measures for the elderly only on the final total number of fatalities (top left); the final total number of fatalities per age group (top right) as well as for the different time course profiles of the total active cases (middle left); reproduction number (R_0) (middle right); the number of critical cases (bottom left) and the number of fatalities (bottom right). Numbers are in percentage of the total population of all ages.

As shown in Figure 3(top left) the selective social isolation of the elderly has a potentially very significant impact on final total fatalities at an almost comparable level than the previous scenario of universal isolation. This is a result with potentially significant consequences as it indicates that a sustained isolation selective only to the elderly and not to the other age groups could alleviate the economic damage at small numbers of increased total fatalities. The decrease in social interactions in schools and colleges by isolation of the young may however have an impact on the overall multiplier of infections from youngsters to adults.

Scenario #3. Selective social isolation of the young

The impact of selective imposed social isolation of those under 20 years old is evaluated in this scenario. The parameter that describes this intervention is the average number of daily social interactions with other people that healthy susceptible individuals of the age groups under 20 years old have (ni_h). In this scenario, isolation measures are applied only to the youngsters. Figure 4 shows the results for this scenario, for the output variables indicated, in absence of other interventions.

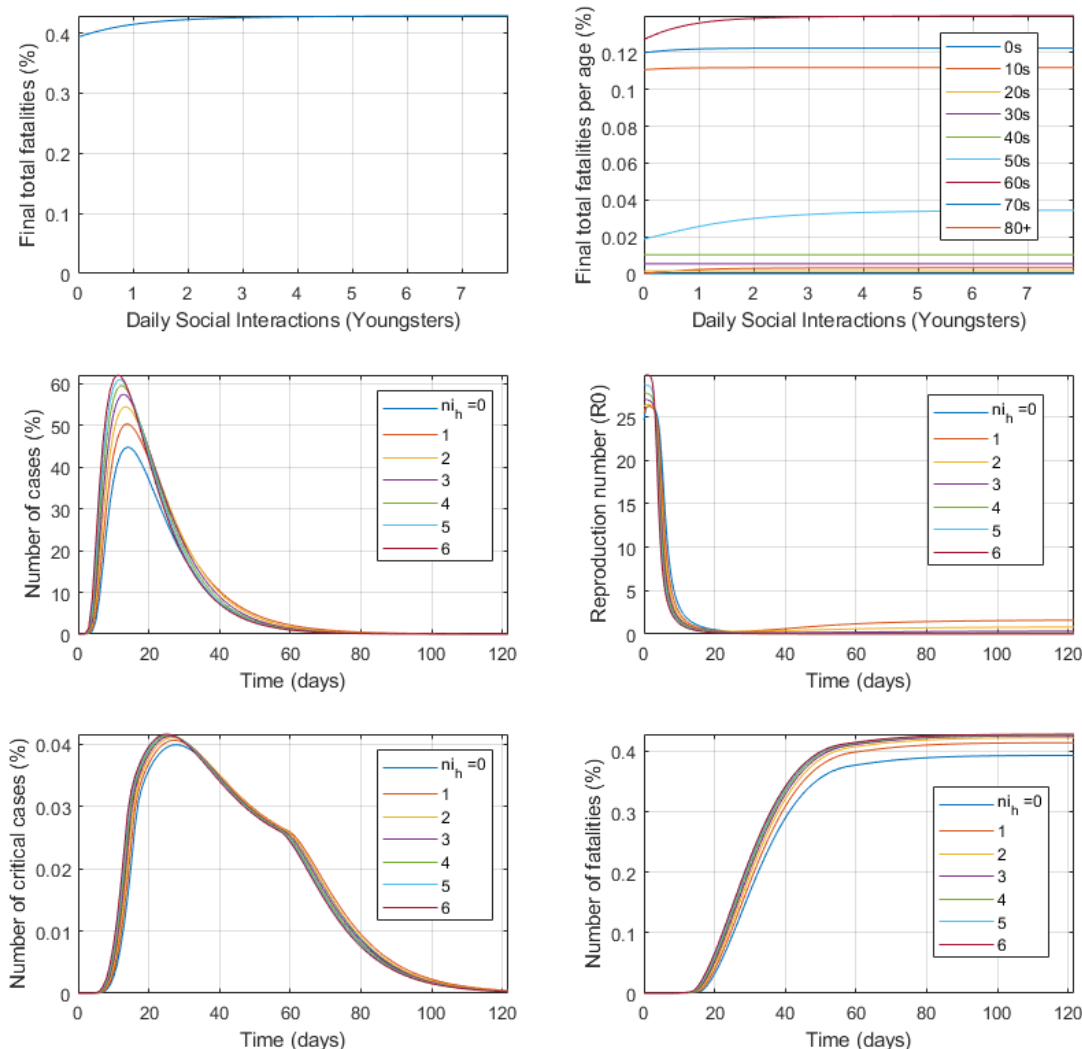


Figure 4. Impact of selective social isolation to the young on the final total number of fatalities (top left); the final number of fatalities per age group (top right) as well as for the different time course profiles of total active cases (middle left); reproduction number (R_0) (middle right); number of critical cases (bottom left) and the number of fatalities (bottom right). Numbers are in percentage of the total population.

The young population have been observed to be quite resistant to the disease. Theoretically at least, young, unaffected lungs tolerate and defend better from the viral load. The isolation of the young produces no effect in the overall final fatality rate but produces a moderate impact on the mortality of the elderly at low values of ni_h . As it can be seen in Figure 4, social isolation of the young has little impact producing almost identical curves for any levels of social isolation. It is thought however that the decrease in social interactions in schools and colleges by isolation of the young may have a large impact on the overall multiplier of infections from youngsters to adults. This emergent aspect of the disease spread behaviour and containment efforts is captured in our results, even though the present model does not incorporate geographical features and does not explicitly describe location-specific population interactions (such as those synthetic location-specific contact patterns in *Prem et al., 2020*).

Scenario #4. Selective social isolation of young and elderly combined

The impact of selective imposed social isolation to both those under 20 and those over 60 years old is evaluated in this scenario. The parameter that describes this intervention is the average number of daily social interactions with other people that healthy susceptible individuals of the age groups under 20 and over 60 years old have (ni_h). In this scenario, the isolation measures are applied selectively only to the youngsters and the elderly. Figure 5 illustrates the model predictions for this scenario, in terms of the output variables indicated, in absence of any other interventions.

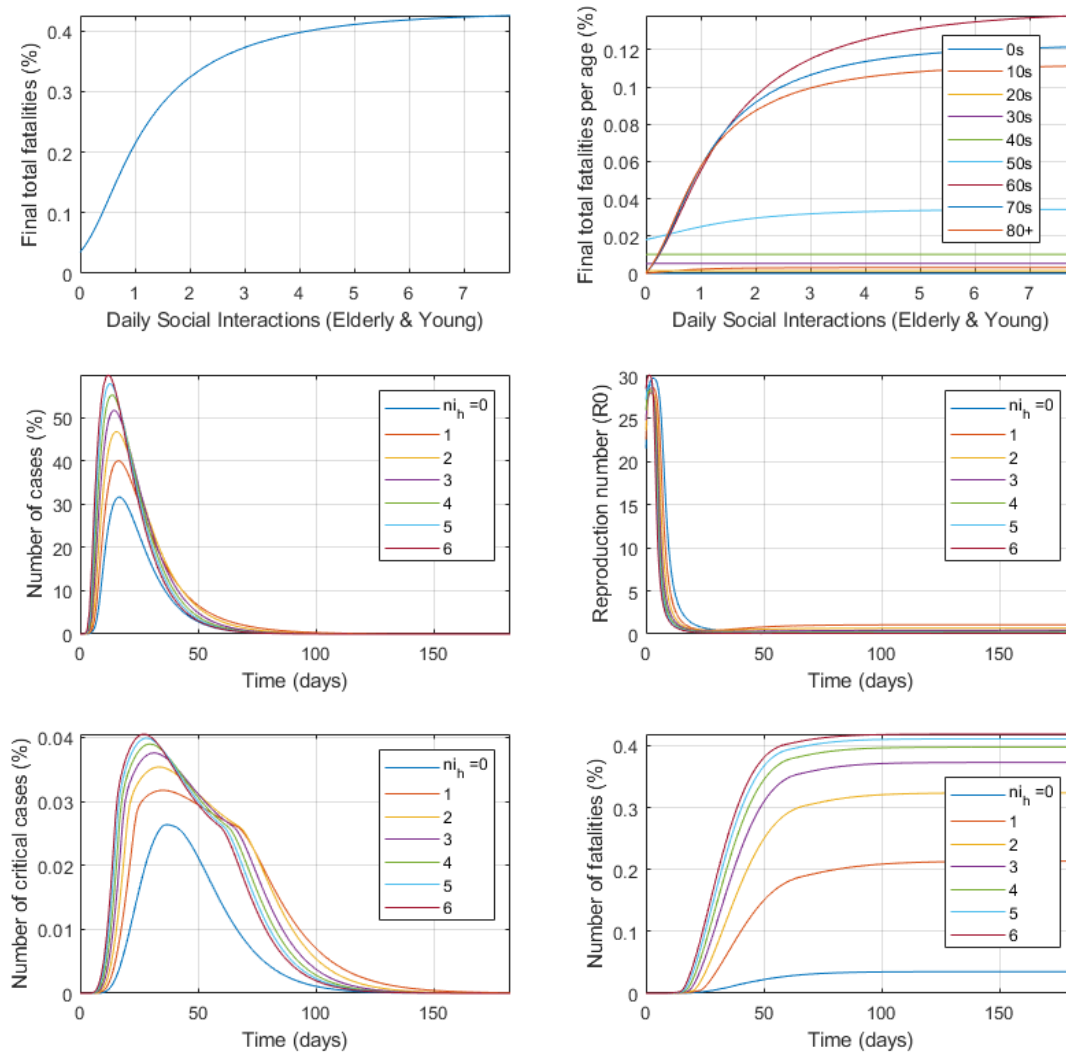


Figure 5. Impact of selective social isolation measures applied to both for the young and the elderly only but not to the rest of the population on the final total number of fatalities (top left); the final total number of fatalities per age group (top right) as well as for the different time course profiles of the total active cases (middle left); reproduction number (R_0) (middle right); the number of critical cases (bottom left) and the number of fatalities (bottom right). Numbers are in percentage of the total population of all ages.

Many of the early interventions during the COVID19 outbreak started by protecting the elderly and isolating the young (no schools, no colleges or universities for students), decreasing the number of interactions of the two subpopulations substantially. The isolation of these population groups together results similarly to that of the isolation of the elderly alone with no significant added value in isolating the young respect to that the elderly alone as shown in Figure 3.

Scenario #5. Increase on critical health care resources

The impact of the availability of intensive care beds is evaluated in this scenario. The parameter that describes this intervention is the number of available intensive care beds per million population. Figure 6 illustrates the model predictions for this scenario, in terms of the output variables indicated, in absence of any other interventions.

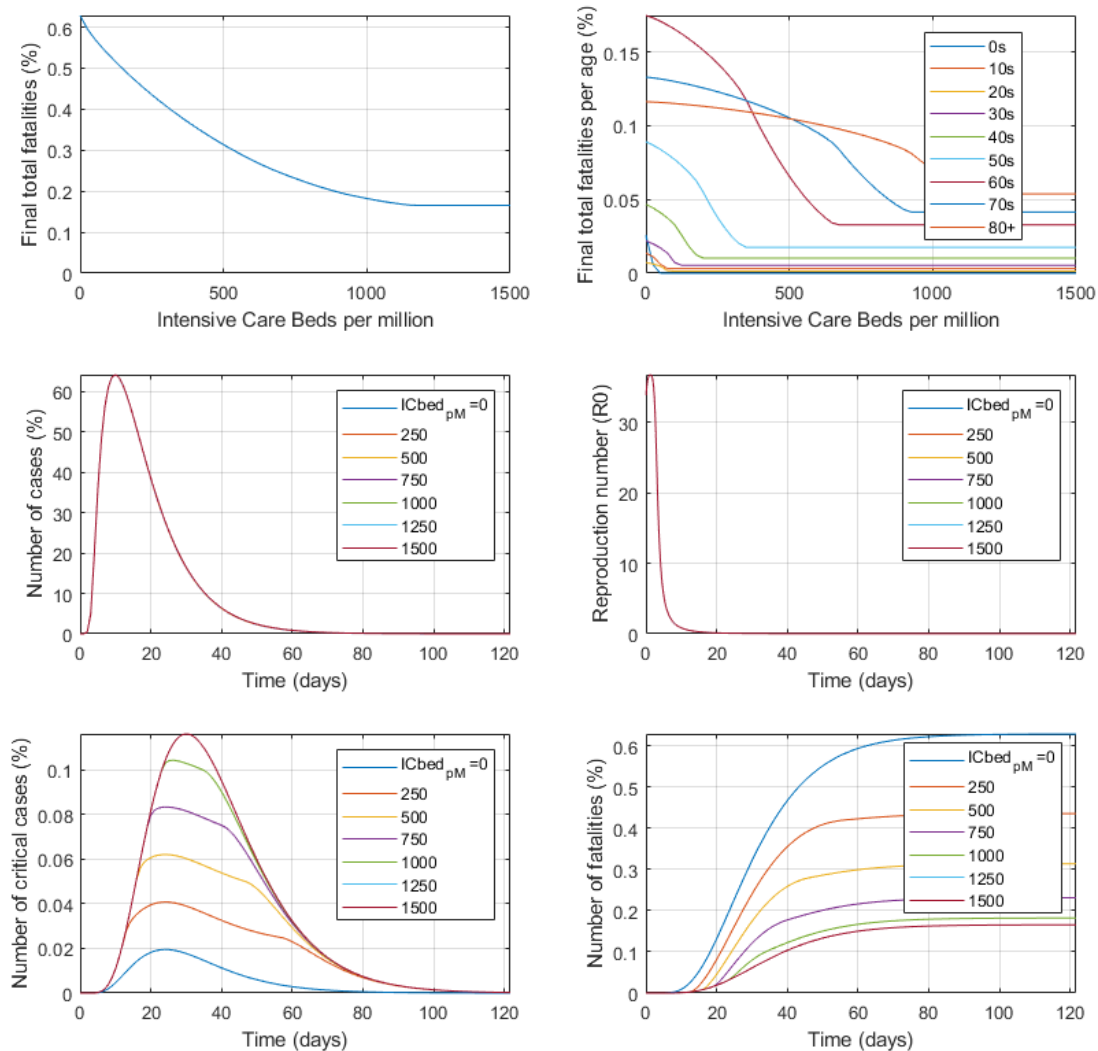


Figure 6. Impact of the availability of intensive care beds on the final total number of fatalities (top left); the final total number of fatalities per age group (top right) as well as for the different time course profiles of the total active cases (middle left); reproduction number (R_0) (middle right); the number of critical cases (bottom left) and the number of fatalities (bottom right). Numbers are in percentage of the total population of all ages.

Figure 6(top left) shows the enormous impact in decreasing total fatalities that the increase in critical care resources can have, the higher the availability of critical beds, the lesser the fatality rate. The trend applies until there is no shortage of IC beds and fatalities are the unavoidable ones. This intervention avoids those deaths that are preventable by the availability of ventilators (mainly) and critical care support. With the current parameter values in a million population it appears that around 8 lives could be saved per additional intensive care bed.

Scenario #6. Increase in personal protective measures

The impact of increased use of PPE and behavioural awareness is evaluated in this scenario. The parameters that describe this intervention is a factor increasing the default values (see Table A3) of the Ipa parameters of the healthy and infected population groups (Ipa_h , Ipa_{ps} and Ipa_s). Increases in these parameters decrease the probability of infection per interaction (see Eqs. 1) and subsequently the rates of infection (Eqs. 2). Figure 7 illustrates the model predictions for this scenario, in terms of the output variables indicated, in absence of any other interventions.

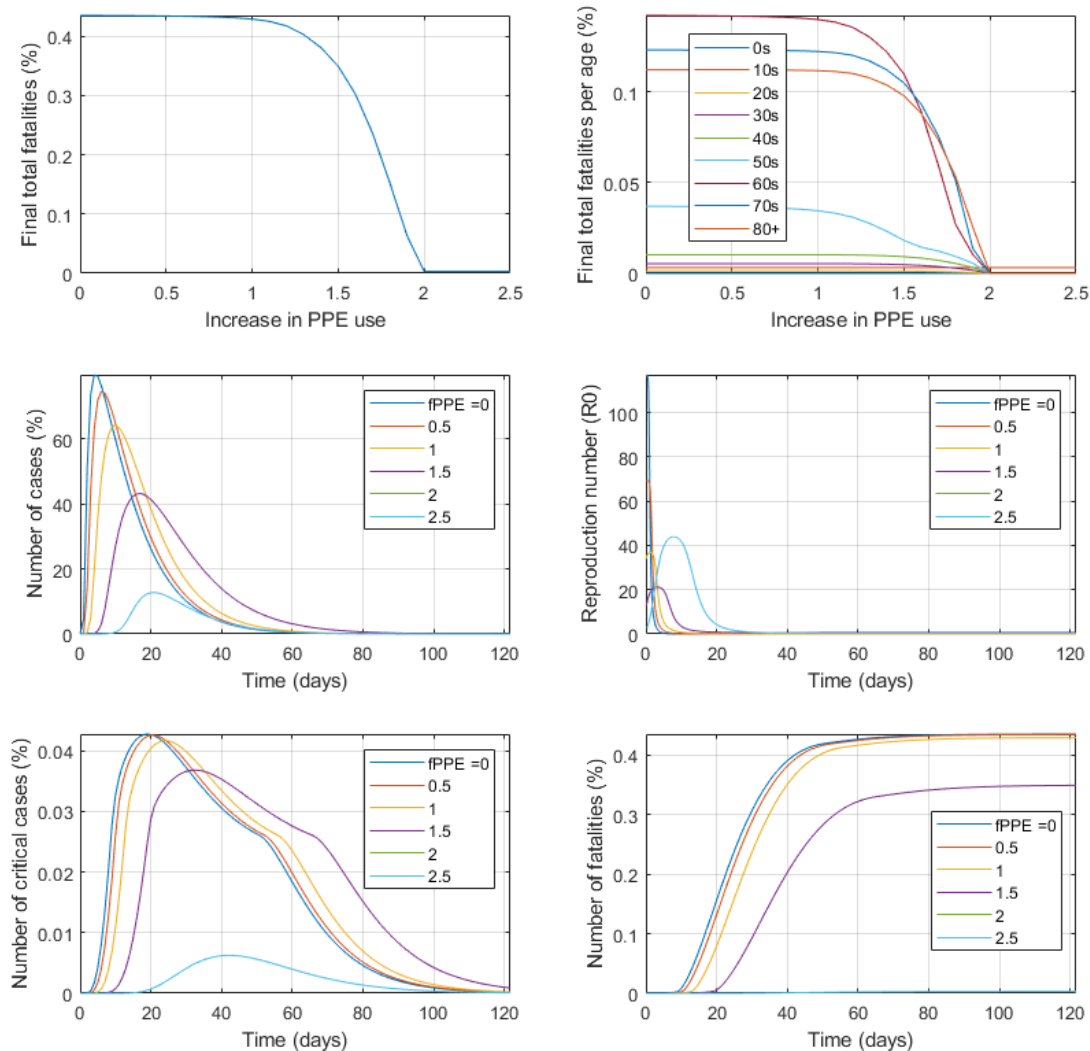


Figure 7. Impact of an increase factor in the use of PPE by both infected and healthy groups respect to the default values (Table A3) on the final total number of fatalities (top left); the final total number of fatalities per age group (top right) as well as for the different time course profiles of the total active cases (middle left); reproduction number (R_0) (middle right); the number of critical cases (bottom left) and the number of fatalities (bottom right). Numbers are in percentage of the total population of all ages.

As it is shown in Figure 7 the extensive use of PPE appears as potentially having a major impact on total outbreak fatalities at the highest levels of protection. There is an inverse relationship between the level of protection and the overall fatality of the disease. The peak of number of cases is reached earlier and is higher if low levels of personal protection, the infectability and R_0 follow the same pattern. The peak number of critical cases is also decreased and slowed through time.

Scenario #7. Awareness of infection by extensive random testing

The impact of increasing the number of tests to all population is evaluated in this scenario. Widespread testing will increase tests done also to both infected pre-symptomatic and symptomatic individuals. The parameter that describes this intervention is a reduction factor in social interactions due to knowledge of infection by PS and S individuals ($r_{fi_{ps}}$ and r_{fi_s}). Reduced values of $r_{fi_{ps}}$ and r_{fi_s} decrease the fraction among of interactions among total from both PS and S (see Eq. 2.a-b) and therefore the rates of infection by these two groups (Eq. 1.a-b). The impact of applying an isolation reduction factor to the default rfi values is evaluated. Figure 8 illustrates the model predictions for this scenario, in terms of the output variables indicated, in absence of any other interventions.

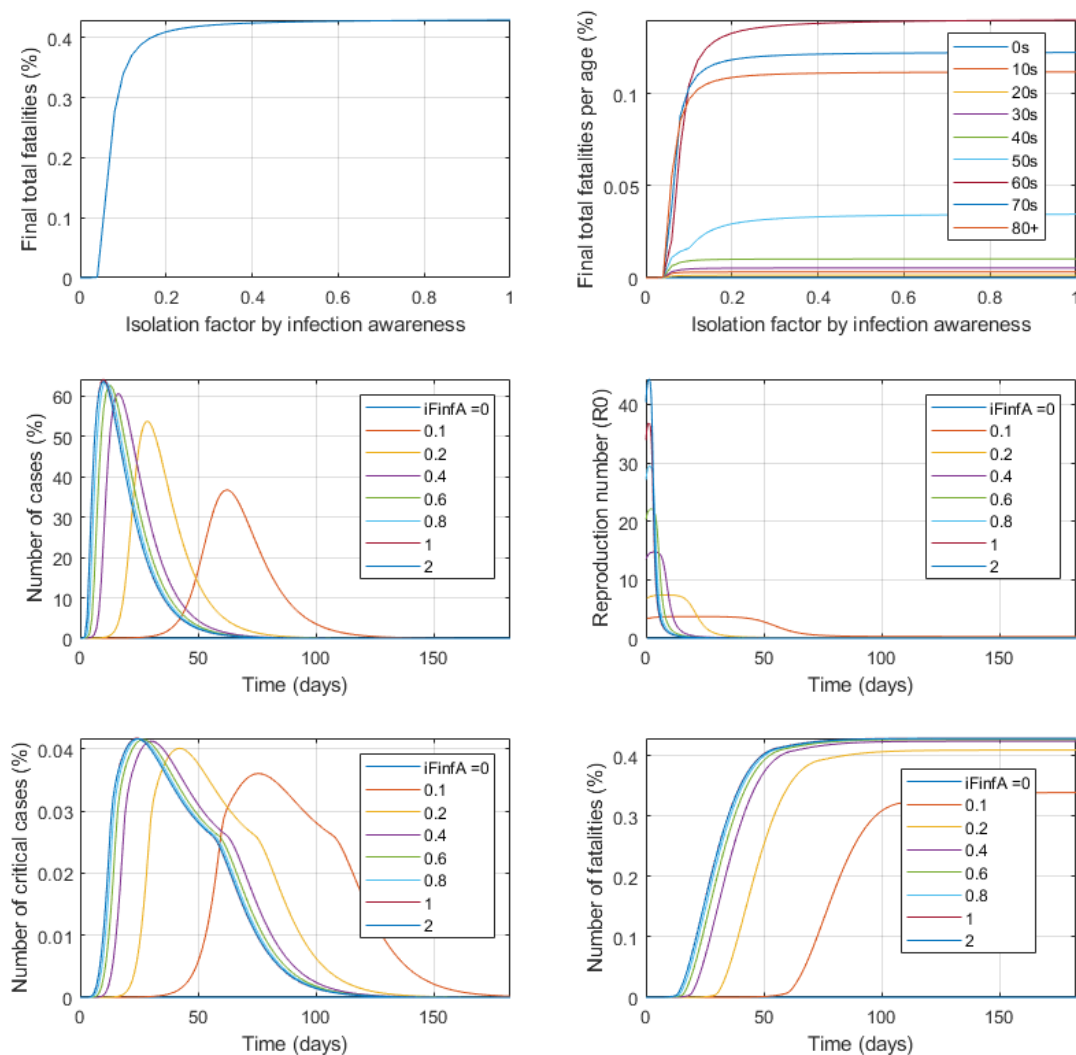


Figure 8. Impact of extensive testing of population and infection awareness of infected pre-symptomatic and symptomatic groups that leads to modified social isolation factor respect to their default rfi values (Table A3), on the final total number of fatalities (top left); the final total number of fatalities per age group (top right) as well as for the different time course profiles of the total active cases (middle left); reproduction number (R_0) (middle right); the number of critical cases (bottom left) and the number of fatalities (bottom right). Numbers are in percentage of the total population of all ages.

The increased awareness of the infected by testing has a great impact and it is a great differentiator among subgroups (no awareness to high awareness) in the number of cases, critical cases and total number of fatalities throughout time. The peaks are significantly decreased by awareness. It is worth noting how the number of fatalities can be brought almost to zero by complete awareness of infection and isolation. Universal testing and isolation, if possible could be one of the great modifiers of the outcome of the outbreak.

Impact of dynamic interventions on a COVID19 outbreak case study

The above static interventions were evaluated in terms of a sustained action over a parameter at different levels and its impact on the outbreak outputs. In outbreaks, aside from the immediate management of needs and resources, the time to return to normal becomes of great concern. In this second section, dynamic interventions are evaluated specifically in terms of the ending of social isolation measures once different threshold values for R_0 (everchanging due to interventions to manage infectability) of the fatality rate are reached. The model dynamic calculation of R_0 allows for the evaluation of the use of this variable as a criterion for the relaxation (or application) of interventions. These dynamic scenarios are considered of potential interest as governments and local authorities must evaluate and decide on when to apply the social distancing and isolation mitigation measures; whether it can be done totally or gradually by subgroups; and the potential impact of ending social isolation will have in further behaviour of the disease spread.

Scenario #8. Complete end of social isolation once R_0 threshold is reached

The impact of ending social isolation upon reaching different threshold values of the R_0 (as a function of all interventions to decrease infectibility) is evaluated in this scenario. This intervention is implemented by starting with initial social isolation in place and average number of daily social interactions (n_{ih}) with value of 1 and returning it back to its default “do nothing” value once the threshold R_0 value is reached. Figure 9 shows the model predictions for this scenario, in terms of the output variables indicated.

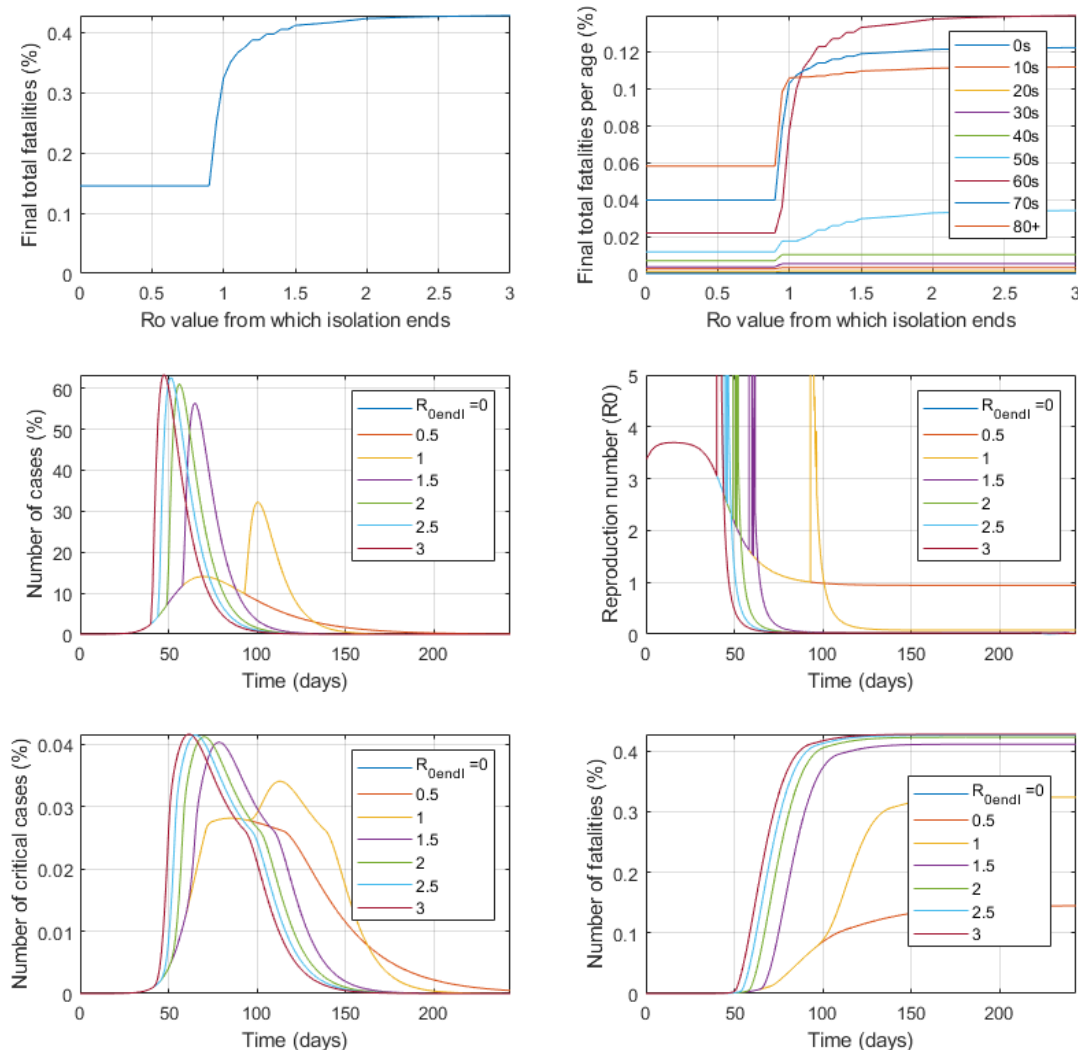


Figure 9. Impact of ending social isolation (n_{ih} from 1 back to 10) upon reaching different threshold values of the R_0 , on the final total number of fatalities (top left); the final total number of fatalities per age group (top right) as well as for the different time course profiles of the total active cases (middle left); reproduction number (R_0) (middle right); the number of critical cases (bottom left) and the number of fatalities (bottom right). Numbers are in percentage of the total population of all ages.

The results in Figure 9(top left) clearly indicate that a withdrawal of isolation measures when R_0 values remain above 1 will lead to little impact on the total fatalities. It is also observed that when isolation is ended even at low threshold R_0 values, increases in the production of new crude number of fatalities and a peak in critical cases occurs after a period of time. These are always accompanied to sudden spike in R_0 for a short period before its collapse. Complete end of isolation may prove to be not the best course of action until R_0 has reached levels of much lower than 1.

Scenario #9. End of social isolation except for elderly once R_0 threshold is reached

The impact of ending social isolation for all, except for those over 60 years old, upon reaching different threshold values of the R_0 is evaluated in this scenario. This intervention is implemented by starting at an initial social isolation in place with a value of 1 for the average number of daily social interactions (n_{ih}) and, once the given threshold R_0 value is reached, returning it back to its default “do nothing” value for all age groups except the elderly. Figure 10 shows the model predictions for this scenario, in terms of the output variables indicated.

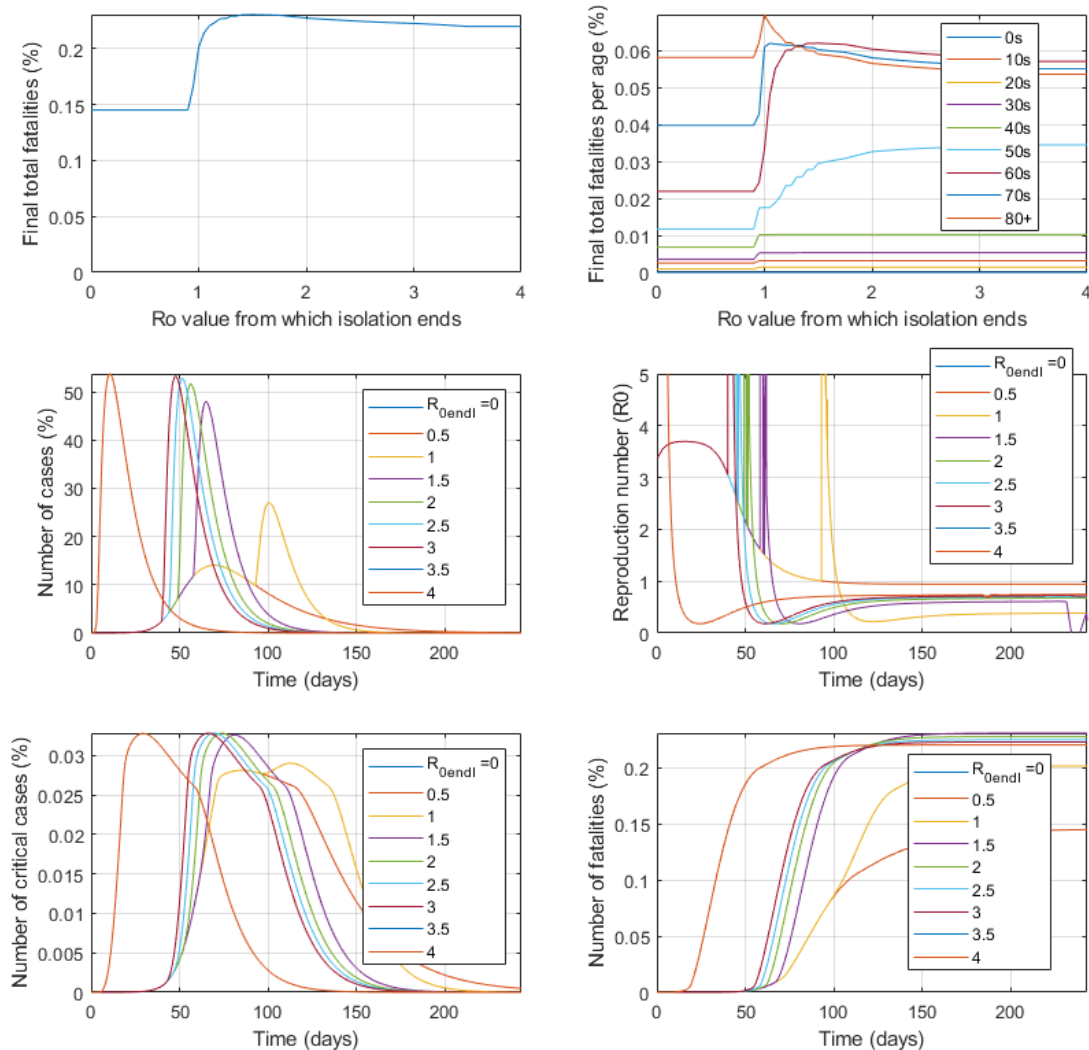


Figure 10. Impact of ending social isolation (n_{ih} from 1 back to 10) for all except the elderly (over 60) upon reaching different threshold values of the R_0 , on the final total number of fatalities (top left); the final total number of fatalities per age group (top right) as well as for the different time course profiles of the total active cases (middle left); reproduction number (R_0) (middle right); the number of critical cases (bottom left) and the number of fatalities (bottom right). Numbers are in percentage of the total population of all ages.

The results in Figure 10(top left) show again that an impact in fatalities will occur if the isolation ends at values of R_0 over 1. The impact of ending social isolation at any R_0 value is in this case smaller as the elderly remain isolated, this is in line with the results obtained in Scenario 2 and shown Figure 3. The decrease of total fatalities of those in the age over 80 observed when isolation ends at, higher than 1, increasing threshold R_0 values, is somehow unexpected.

Scenario #10. End of social isolation once fatality rate threshold is reached

The impact of ending social isolation upon reaching different threshold values of the daily fatality rate (after it has passed its maximum) is evaluated in this scenario. The daily fatality rate is selected instead of e.g. the number of cases because it can be much more exactly assessed (incontrovertible as opposed to the number of cases). The decrease in the fatality rate is usually reached after the decrease in number of cases (“over the peak”) as shown by most epidemiological curves for COVID-19 published so far. This intervention is implemented by starting at an initial social isolation in place with a value of 1 for the average number of daily social interactions (n_{ih}) and returning it back to its default “do nothing” value when, after the rate passed its maximum, the given threshold value of the rate is reached. Figure 11 shows the results for this scenario for the output variables indicated.

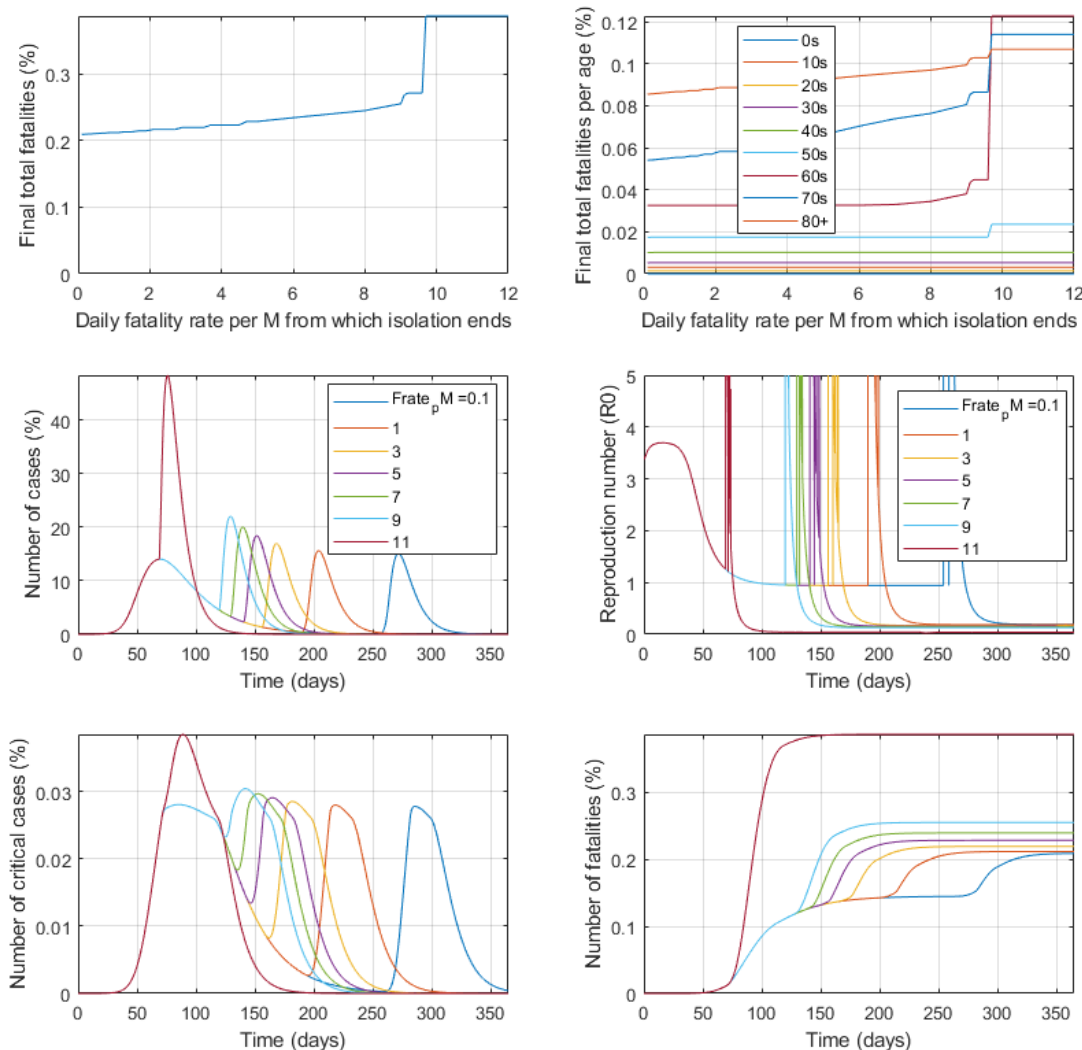


Figure 11. Impact of ending social isolation (n_{ih} from 1 back to 10) once the fatality rate, after surpassing its maximum, reaches different threshold values, on the final total number of fatalities (top left); the final total number of fatalities per age group (top right) as well as for the different time course profiles of the total active cases (middle left); reproduction number (R_0) (middle right); the number of critical cases (bottom left) and the number of fatalities (bottom right). Numbers are as percentage of total population.

In this scenario all social isolation are ended once the fatality rate reaches a threshold after it started declining. As shown in Figure 11 it appears to be a very narrow threshold from which the isolation measures can be withdrawn with low impact on total fatality. If measures are ended just before the threshold is reached the overall fatality rate and the fatality rate for elders rises sharply. For values below that threshold a still a decrease in total fatalities can be obtained if lower thresholds of fatality rate for isolation end are used.

Scenario #11. End of social isolation except for elderly once fatality rate threshold is reached

The impact of ending social isolation for all, except for those under 60 years old, upon reaching different threshold values of the fatality rate, after it reaching its maximum, is evaluated in this scenario. This intervention is implemented by starting at an initial social isolation in place with a value of 1 for the average number of daily social interactions (n_{ih}) and returning it back to its default “do nothing” value, for all age groups except the elderly, once, after the fatality rate reached its maximum, the given threshold value of the rate is reached. Figure 12 shows the model predictions for this scenario, in terms of the output variables indicated.

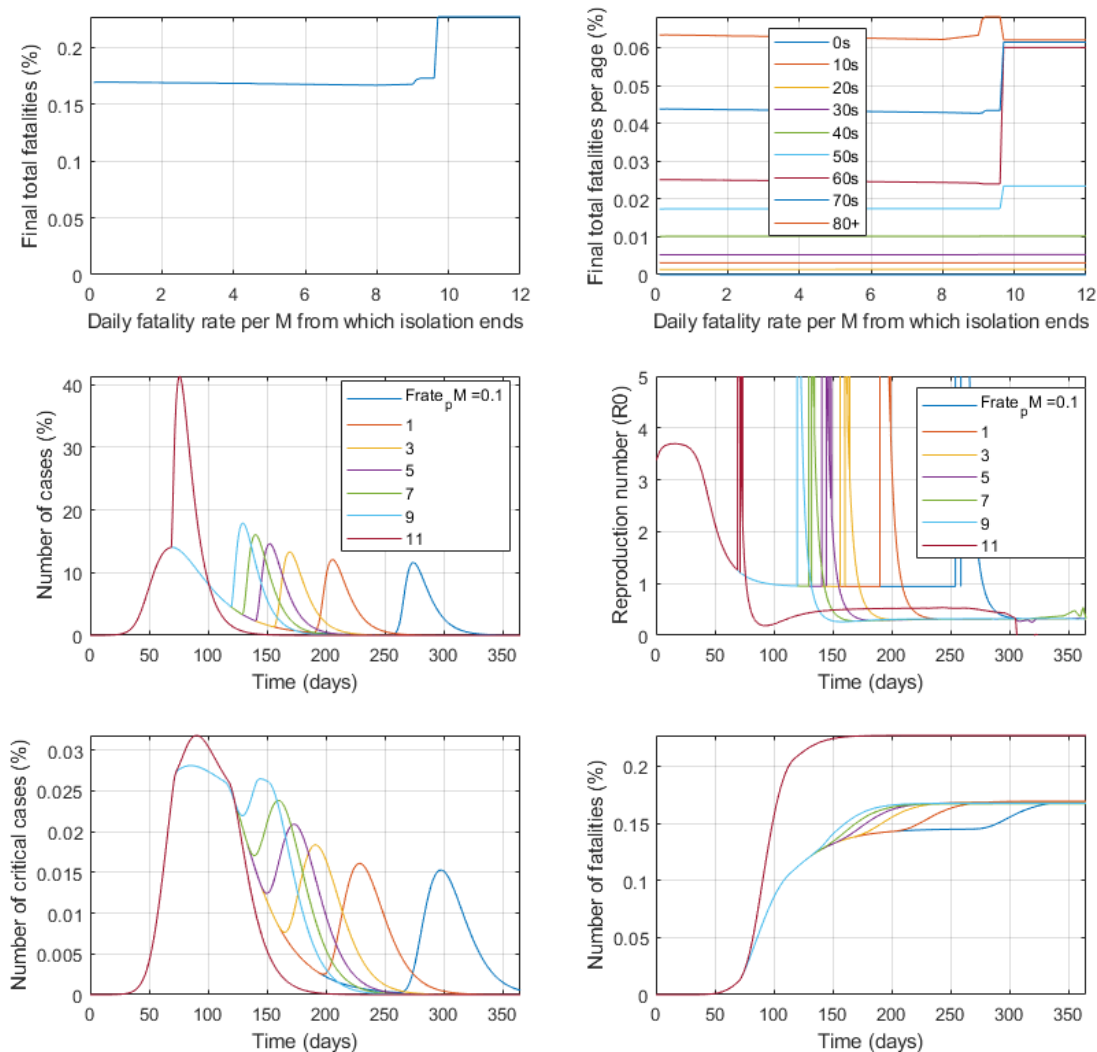


Figure 12. Impact of ending social isolation (n_{ih} from 1 back to 10) once the fatality rate, after surpassing its maximum, reaches different threshold values, on the final total number of fatalities (top left); the final total number of fatalities per age group (top right) as well as for the different time course profiles of the total active cases (middle left); reproduction number (R_0) (middle right); the number of critical cases (bottom left) and the number of fatalities (bottom right). Numbers are as percentage of total population.

In this scenario all social isolation, except of that for the elderly, ends once the fatality rate reaches a threshold after it is already declining. As shown in Figure 12, and analogous to the previous scenario, it appears to be a very narrow threshold from which the isolation measures can be withdrawn with low impact on total fatality. Also, if measures are ended just before the threshold is reached, the overall fatality rate rises sharply similarly. For values below that threshold however here no decrease in total fatalities is predicted when using lower thresholds of the fatality rate to end isolation. These results are also consistent with the idea that isolation of the age groups more vulnerable to the disease should be maintained.

Conclusions on the impact of interventions

The impact of specific interventions on the outbreak time course, number of cases and outcome of fatalities were evaluated. Data available from the COVID19 outbreak as of early April 2020 was used. Our preliminary results for scenarios above and parameter values used indicate that:

1. Universal social isolation measures may be effective in reducing total fatalities only if they are strict and the average number of daily social interactions is reduced to very low numbers.
2. Selective isolation of only the age groups most vulnerable to the disease (i.e. older than 60) appears almost as effective in reducing total fatalities but at a much lower economic damage. The comparison between impacts of social isolation interventions to all or selective by age on the final total number of fatalities (Figure 13) shows that the isolation of the elderly can achieve equivalent impact to that of all.
3. An increase in the number of critical care beds could save up significant numbers of lives. Using our current parameters values, for a one million population, an estimate of 8 fatalities could be avoided per extra available critical care unit.
4. The use of protective equipment (PPE) appears capable of very significantly reducing total fatalities if implemented extensively and to a high degree;
5. Extensive random testing of the population leading to infection recognition and subsequent immediate (self) isolation of the infected individuals, can dramatically reduce the total fatalities but only if implemented to almost the entire population and sustained over time.
6. Ending isolation measures with R_0 above one (with a safety factor) appears to renders the previous isolation measures useless as fatality rate eventually reaches values close to if nothing was ever done;
7. Ending isolation measures only for the population under 60 y/o with R_0 values still above one increases total fatalities but only around half as much as if isolation is ended for everyone.
8. A threshold value for daily fatality rate (equivalent to the R_0 below one) appears to exist for the feasible end of isolation measures. Daily fatality rates are known very accurately unlike the R_0 and could be used criteria for intervention. In Figure 14 the impacts on total final number of fatalities of the withdrawal of social isolation from threshold values for (R_0) and of daily fatality rate per million people are shown. A comparison between the cases when withdrawal is done universally or restricted only to those under 60 years old is shown.

It is important to note that any interpretation of the above results for the COVID19 outbreak interventions must be considered only qualitatively at this stage due to the low confidence (lack of complete and valid data) on the parameter values available at the time of writing. Any quantitative interpretation of the results must be accompanied with a critical discussion in terms of the model limitations and its frame of application. Next immediate steps involve the sensitivity analysis of the parameters with the lowest confidence. A roadmap for model expansion and broader implementation is discussed below.

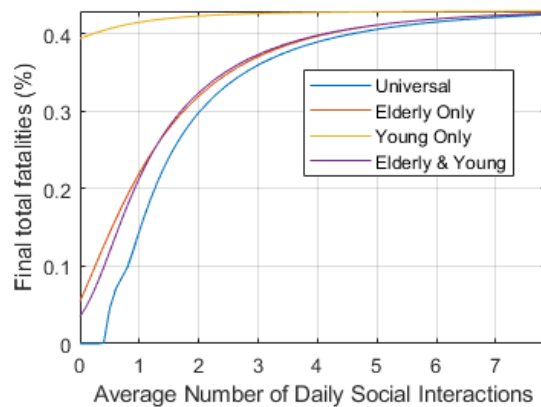


Figure 13. Comparison between impacts of social isolation interventions to all or selective by age on the final total number of fatalities.

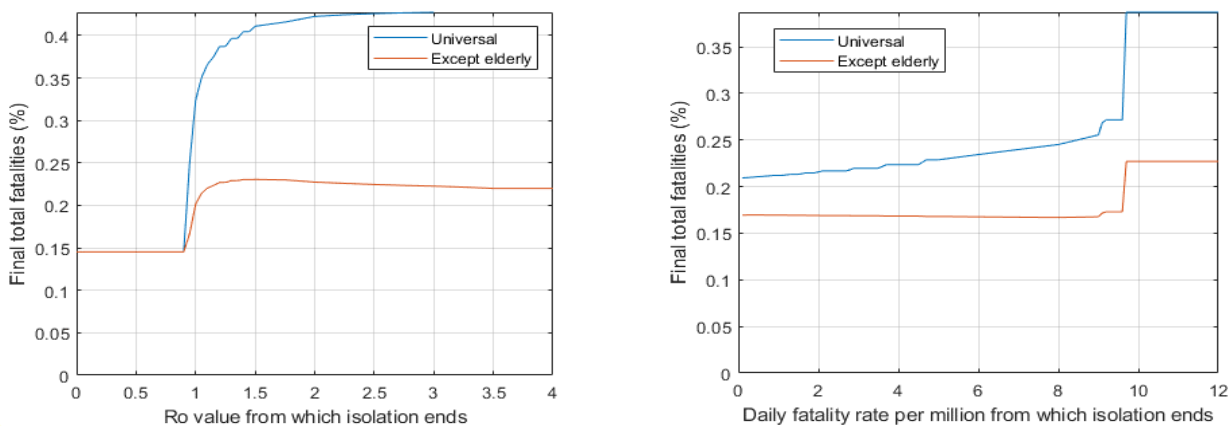


Figure 14. Impacts on total final number of fatalities of the withdrawal of social isolation from threshold values for (R_0) (left) and of daily fatality rate per million people (right). Comparison between impacts when withdrawal is universal or only to those under 60 years old.

Roadmap for model expansion and application

The model requires parameter calibration against valid data from representative populated cities. Data from cities in which population is typically very interconnected socially in public areas and public transport is widely used, are particularly suited for calibration of this model.

The model in its current version would benefit from more detailed descriptions and sub models of some of the intervention relevant parameters such as the levels of social interaction and personal protection measures.

The model modularity and its fast computation allows for its easy scale up into multiple population nucleus that could be simulated in parallel with degrees of interconnectivity among them. Separate independent copies of the model can be run in parallel one for e.g. each city in a region or country and migration terms can be added between cities. Interventions can then be defined to include e.g. travel restrictions between those cities at different levels.

The mechanistic nature of the model makes it also very suitable for the evaluation of advanced optimisation and optimum control strategies. Its capacity of describing complex interactions makes it also of potentially great use to develop advanced artificial intelligence (AI) algorithms to aide and provide advice to authorities during decision making. AI algorithms could be trained by evaluation of very large numbers of scenarios combining static and dynamic interventions of different types against total fatalities and economic damage.

Supplementary Information and source code

The for Matlab® source code and Excel file containing all parameter values used as well as a non-age segregated version of the model are available at https://github.com/EnvBioProM/COVID_Model

Acknowledgements

All authors wish to thank Khalifa University and the Government of Abu Dhabi for the funding and support.

References

- Anderson, R. M., Anderson, B., & May, R. M. (1992). *Infectious diseases of humans: dynamics and control*. Oxford university press.
- Balcan, D., Gonçalves, B., Hu, H., Ramasco, J. J., Colizza, V., & Vespignani, A. (2010). Modeling the spatial spread of infectious diseases: The GLObal Epidemic and Mobility computational model. *Journal of computational science*, 1(3), 132-145.
- Bendix A. (2020) A day-by-day breakdown of coronavirus symptoms shows how the disease, COVID-19, goes from bad to worse. *Business Insider* (last accessed 30-3-2020)
<https://www.businessinsider.com/coronavirus-covid19-day-by-day-symptoms-patients-2020-2>
- Berezovskaya, F., Karev, G., Song, B., & Castillo-Chavez, C. (2005). A simple epidemic model with surprising dynamics. *Mathematical Biosciences & Engineering*, 2(1), 133.
- Bettencourt, L. M., & Ribeiro, R. M. (2008). Real time bayesian estimation of the epidemic potential of emerging infectious diseases. *PLoS One*, 3(5).
- Biggerstaff, M., Cauchemez, S., Reed, C., Gambhir, M., & Finelli, L. (2014). Estimates of the reproduction number for seasonal, pandemic, and zoonotic influenza: a systematic review of the literature. *BMC infectious diseases*, 14(1), 480.
- Brauer, F., Castillo-Chavez, C., & Castillo-Chavez, C. (2012). *Mathematical models in population biology and epidemiology* (Vol. 2). New York: Springer.
- Britton, T. (2010). Stochastic epidemic models: a survey. *Mathematical biosciences*, 225(1), 24-35.
- Capasso, V., & Wilson, R. E. (1997). Analysis of a reaction-diffusion system modelling man-environment-man epidemics. *SIAM Journal on Applied Mathematics*, 57(2), 327-346.
- Chinazzi, M., Davis, J.T., Ajelli, M., Gioannini, C., Litvinova, M., Merler, S., y Piontti, A.P., Mu, K., Rossi, L., Sun, K. and Viboud, C. (2020). The effect of travel restrictions on the spread of the 2019 novel coronavirus (COVID-19) outbreak. *Science*. 06 Mar 2020:eaba9757
- Chowell, G., Luo, R., Sun, K., Roosa, K., Tariq, A., & Viboud, C. (2020). Real-time forecasting of epidemic trajectories using computational dynamic ensembles. *Epidemics*, 30, 100379.
- Chowell, G., Sattenspiel, L., Bansal, S., & Viboud, C. (2016). Mathematical models to characterize early epidemic growth: A review. *Physics of life reviews*, 18, 66-97.
- Colizza, V., Barrat, A., Barthélemy, M., & Vespignani, A. (2006). The role of the airline transportation network in the prediction and predictability of global epidemics. *Proceedings of the National Academy of Sciences*, 103(7), 2015-2020.
- Cooper, B. S., Pitman, R. J., Edmunds, W. J., & Gay, N. J. (2006). Delaying the international spread of pandemic influenza. *PLoS medicine*, 3(6).
- Delamater, P. L., Street, E. J., Leslie, T. F., Yang, Y., & Jacobsen, K. H. (2019). Complexity of the Basic Reproduction Number (R_0). *Emerging Infectious Diseases*, 25(1), 1-4.
<https://dx.doi.org/10.3201/eid2501.171901>.
- Dong, E., Du, H., & Gardner, L. (2020). An interactive web-based dashboard to track COVID-19 in real time. *The Lancet Infectious Diseases*.
- Fenichel, E.P., Castillo-Chavez, C., Ceddia, M.G., Chowell, G., Parra, P.A.G., Hickling, G.J., Holloway, G., Horan, R., Morin, B., Perrings, C. and Springborn, M. (2011). Adaptive human behavior in epidemiological models. *Proceedings of the National Academy of Sciences*, 108(15), 6306-6311.

- Ferguson NM *et al.* (2020) Impact of non-pharmaceutical interventions (NPIs) to reduce COVID19 mortality and healthcare demand. <https://spiral.imperial.ac.uk/handle/10044/1/77482>
- Ferguson, N. M., Cummings, D. A., Fraser, C., Cajka, J. C., Cooley, P. C., & Burke, D. S. (2006). Strategies for mitigating an influenza pandemic. *Nature*, 442(7101), 448-452.
- Flaxman S, Mishra S, Gandy A *et al.* (2020) Estimating the number of infections and the impact of nonpharmaceutical interventions on COVID-19 in 11 European countries. Imperial College London
- Flaxman, S. *et al.* (2020) Report 13: Estimating the number of infections and the impact of non-pharmaceutical interventions on COVID-19 in 11 European countries. Imperial College London
- Funk, S., Gilad, E., Watkins, C., & Jansen, V. A. (2009). The spread of awareness and its impact on epidemic outbreaks. *Proceedings of the National Academy of Sciences*, 106(16), 6872-6877.
- Gomes, M. F., y Piontti, A. P., Rossi, L., Chao, D., Longini, I., Halloran, M. E., & Vespignani, A. (2014). Assessing the international spreading risk associated with the 2014 West African Ebola outbreak. *PLoS currents*, 6.
- González-Peñas H, Lu-Chau T, LemaJM and Rodríguez J (2020) A microbial population dynamics model for the Acetone-Butanol-Ethanol fermentation process. *Authorea*. February 22, 2020. DOI: <https://doi.org/10.22541/au.158240035.50698760>
- Grassly, N. C., & Fraser, C. (2008). Mathematical models of infectious disease transmission. *Nature Reviews Microbiology*, 6(6), 477-487.
- Gray, A., Greenhalgh, D., Hu, L., Mao, X., & Pan, J. (2011). A stochastic differential equation SIS epidemic model. *SIAM Journal on Applied Mathematics*, 71(3), 876-902.
- Hall, I. M., Gani, R., Hughes, H. E., & Leach, S. (2007). Real-time epidemic forecasting for pandemic influenza. *Epidemiology & Infection*, 135(3), 372-385.
- Hellewell, J., Abbott, S., Gimma, A., Bosse, N.I., Jarvis, C.I., Russell, T.W., Munday, J.D., Kucharski, A.J., Edmunds, W.J., Sun, F. and Flasche, S. (2020). Feasibility of controlling COVID-19 outbreaks by isolation of cases and contacts. *The Lancet Global Health*.
- Henze, M., Gujer, W., Mino, T., & van Loosdrecht, M. C. (2000). Activated sludge models ASM1, ASM2, ASM2d and ASM3. IWA publishing.
- Hethcote, H. W. (2000). The mathematics of infectious diseases. *SIAM review*, 42(4), 599-653.
- Hu, Z., Song, C., Xu, C., Jin, G., Chen, Y., Xu, X., Ma, H., Chen, W., Lin, Y., Zheng, Y., *et al.* (2020). Clinical characteristics of 24 asymptomatic infections with COVID-19 screened among close contacts in Nanjing, China. *Sci China Life Sci* 63, <https://doi.org/10.1007/s11427-020-1661-4>
- INE Spain (2020) <https://www.ine.es/> (last accessed 31/3/2020)
- Keeling, M. J., & Eames, K. T. (2005). Networks and epidemic models. *Journal of the Royal Society Interface*, 2(4), 295-307.
- Keeling, M. J., & Rohani, P. (2008). *Modeling infectious diseases in humans and animals*. Princeton University Press.
- Kermack, W. O., & McKendrick, A. G. (1927). A contribution to the mathematical theory of epidemics. *Proceedings of the Royal Society of London. Series A, Containing papers of a mathematical and physical character*, 115(772), 700-721.
- Kucharski, A.J., Russell, T.W., Diamond, C., Liu, Y., Edmunds, J., Funk, S., Eggo, R.M., Sun, F., Jit, M., Munday, J.D. and Davies, N. (2020). Early dynamics of transmission and control of COVID-19: a mathematical modelling study. *The lancet infectious diseases*.
- Lauer, S.A., Grantz, K.H., Bi, Q., Jones, F.K., Zheng, Q., Meredith, H.R., Azman, A.S., Reich, N.G. and Lessler, J. (2020). The incubation period of coronavirus disease 2019 (COVID-19) from publicly reported confirmed cases: estimation and application. *Annals of internal medicine*.
- Lee, B. Y., Haidari, L. A., & Lee, M. S. (2013). Modelling during an emergency: the 2009 H1N1 influenza pandemic. *Clinical Microbiology and Infection*, 19(11), 1014-1022.
- Li, J., Zhou, Y., Ma, Z., & Hyman, J. M. (2004). Epidemiological models for mutating pathogens. *SIAM Journal on Applied Mathematics*, 65(1), 1-23.

- Liu, Y., Gayle, A. A., Wilder-Smith, A., & Rocklöv, J. (2020). The reproduction number of COVID-19 is higher compared to SARS coronavirus. *Journal of travel medicine*.
- May, R. M., & Anderson, R. M. (1979). Population biology of infectious diseases: Part II. *Nature*, 280(5722), 455-461.
- McCallum, H., Barlow, N., & Hone, J. (2001). How should pathogen transmission be modelled?. *Trends in ecology & evolution*, 16(6), 295-300.
- Miller, J. C., Slim, A. C., & Volz, E. M. (2012). Edge-based compartmental modelling for infectious disease spread. *Journal of the Royal Society Interface*, 9(70), 890-906.
- Ministerio de Sanidad de España. Actualización nº64: enfermedad por SARS-CoV-2 (COVID-19) 03.04.2020 https://www.mscbs.gob.es/profesionales/saludPublica/ccayes/alertasActual/nCov-China/documentos/Actualizacion_64_COVID-19.pdf
- Murray, C. J., & Lopez, A. D. (1997a). Mortality by cause for eight regions of the world: Global Burden of Disease Study. *The Lancet*, 349(9061), 1269-1276.
- Murray, C. J., & Lopez, A. D. (1997b). Regional patterns of disability-free life expectancy and disability-adjusted life expectancy: Global Burden of Disease Study. *The Lancet*, 349(9062), 1347-1352.
- Murray, C. J., & Lopez, A. D. (1997c). Global mortality, disability, and the contribution of risk factors: Global Burden of Disease Study. *The Lancet*, 349(9063), 1436-1442.
- Murray, C. J., & Lopez, A. D. (1997d). Alternative projections of mortality and disability by cause 1990–2020: Global Burden of Disease Study. *The Lancet*, 349(9064), 1498-1504.
- Newman ME (2003). The structure and function of complex networks. *SIAM review*, 45(2), 167-256.
- Nishiura H, Kobayashi T, Suzuki A, Jung S-Mok, Hayashi K, Kinoshita R, Yang Y, Yuan B, Akhmetzhanov AR, Linton NM, Miyama T (2020) Estimation of the asymptomatic ratio of novel coronavirus infections (COVID-19), *International Journal of Infectious Diseases*, doi:<https://doi.org/10.1016/j.ijid.2020.03.020>
- Nishiura, H. (2011). Real-time forecasting of an epidemic using a discrete time stochastic model: a case study of pandemic influenza (H1N1-2009). *Biomedical engineering online*, 10(1), 15.
- Nishiura, H., Chowell, G., & Castillo-Chavez, C. (2011). Did modeling overestimate the transmission potential of pandemic (H1N1-2009)? Sample size estimation for post-epidemic seroepidemiological studies. *Plos one*, 6(3).
- Nsoesie, E. O., Brownstein, J. S., Ramakrishnan, N., & Marathe, M. V. (2014). A systematic review of studies on forecasting the dynamics of influenza outbreaks. *Influenza and other respiratory viruses*, 8(3), 309-316.
- Pastor-Satorras, R., Castellano, C., Van Mieghem, P., & Vespignani, A. (2015). Epidemic processes in complex networks. *Reviews of modern physics*, 87(3), 925.
- Plimpton, S., & Root, J. (1994). Materials and strategies that work in low literacy health communication. *Public Health Reports*, 109(1), 86.
- Prem, K., Liu, Y., Russell, T.W., Kucharski, A.J., Eggo, R.M., Davies, N., Flasche, S., Clifford, S., Pearson, C.A., Munday, J.D. and Abbott, S. (2020). The effect of control strategies to reduce social mixing on outcomes of the COVID-19 epidemic in Wuhan, China: a modelling study. *The Lancet Public Health*.
- Ramkrishna D and Singh MR (2014) Population Balance Modeling: Current Status and Future Prospects. *Annual Review of Chemical and Biomolecular Engineering* 5:1, 123-146.
- Reluga, T. C. (2010). Game theory of social distancing in response to an epidemic. *PLoS computational biology*, 6(5).
- Riley, S. (2007). Large-scale spatial-transmission models of infectious disease. *Science*, 316(5829), 1298-1301.
- Rivers, C., Chretien, J.P., Riley, S., Pavlin, J.A., Woodward, A., Brett-Major, D., Berry, I.M., Morton, L., Jarman, R.G., Biggerstaff, M. and Johansson, M.A. (2019). Using “outbreak science” to strengthen the use of models during epidemics. *Nature communications*, 10(1), 1-3.
- Roosa, K., Lee, Y., Luo, R., Kirpich, A., Rothenberg, R., Hyman, J.M., Yan, P. and Chowell, G. (2020). Real-time forecasts of the COVID-19 epidemic in China from February 5th to February 24th, 2020. *Infectious Disease Modelling*, 5, 256-263.

- Ruan, S., & Wang, W. (2003). Dynamical behavior of an epidemic model with a nonlinear incidence rate. *Journal of Differential Equations*, 188(1), 135-163.
- Russell TW *et al.* (2020) Using a delay-adjusted case fatality ratio to estimate under-reporting. https://cmmid.github.io/topics/covid19/severity/global_cfr_estimates.html (last access 02/04/2020)
- Siettos, C. I., & Russo, L. (2013). Mathematical modeling of infectious disease dynamics. *Virulence*, 4(4), 295-306.
- Squiers, L., Peinado, S., Berkman, N., Boudewyns, V., & McCormack, L. (2012). The health literacy skills framework. *Journal of health communication*, 17(sup3), 30-54.
- Stephen A. Lauer, Kyra H. Grantz, Qifang Bi, Forrest K. Jones, Qulu Zheng, Hannah R. Meredith, Andrew S. Azman, Nicholas G. Reich, Justin Lessler (2020) The Incubation Period of Coronavirus Disease 2019 (COVID-19) From Publicly Reported Confirmed Cases: Estimation and Application. *Annals of Internal Medicine*, DOI: 10.7326/M20-0504
- Tizzoni, M., Bajardi, P., Poletto, C., Ramasco, J.J., Balcan, D., Gonçalves, B., Perra, N., Colizza, V. and Vespignani, A. (2012). Real-time numerical forecast of global epidemic spreading: case study of 2009 A/H1N1pdm. *BMC medicine*, 10(1), 165..
- Wang, W., & Zhao, X. Q. (2012). Basic reproduction numbers for reaction-diffusion epidemic models. *SIAM Journal on Applied Dynamical Systems*, 11(4), 1652-1673.
- WHO Ebola Response Team. (2014). Ebola virus disease in West Africa—the first 9 months of the epidemic and forward projections. *New England Journal of Medicine*, 371(16), 1481-1495.
- Yang, X. S. (2014). *Nature-inspired optimization algorithms*. Elsevier.
- Zarcadoolas, C. (2011). The simplicity complex: exploring simplified health messages in a complex world. *Health promotion international*, 26(3), 338-350.
- Zhang, Q., Sun, K., Chinazzi, M., y Piontti, A.P., Dean, N.E., Rojas, D.P., Merler, S., Mistry, D., Poletti, P., Rossi, L. and Bray, M. (2017). Spread of Zika virus in the Americas. *Proceedings of the National Academy of Sciences*, 114(22), E4334-E4343.
- Zhou F, Yu T, Du R, *et al.* (2020) Clinical course and risk factors for mortality of adult inpatients with COVID-19 in Wuhan, China: a retrospective cohort study. *Lancet* published online March 9. [http://dx.doi.org/10.1016/S0140-6736\(20\)30566-3](http://dx.doi.org/10.1016/S0140-6736(20)30566-3).

Appendix II. Data sources for the epidemiological and clinical parameters: COVID19 case study

Table A2. Data sources and level of confidence assigned to the epidemiological and clinical parameters from Table A1 for the COVID19 outbreak case study.

Parameter	Sources and details of estimation	Confidence Level
f_{hn_t}	Estimated (no basis)	VL
$f_{s_{ps}}$	Nishiura <i>et al.</i> , 2020	L
f_{sh_s}	Ministerio Sanidad de España: Act. 64 COVID19; Russell <i>et al.</i> (2020)	VL
$f_{sc_{sh}}$	Ferguson <i>et al.</i> (2020)	M
$f_{d_{sc}}$	Ministerio Sanidad España: Act. 64 COVID19; Ferguson <i>et al.</i> (2020)	M
$f_{r_{ps}}$	Calculated ($1 - f_{s_{ps}}$)	M
f_{r_s}	Calculated ($1 - f_{sh_s}$)	M
$f_{r_{sh}}$	Calculated ($1 - f_{sc_{sh}}$)	M
$f_{r_{sc}}$	Calculated ($1 - f_{d_{sc}}$)	M
$t_{s_{ps}}$	Lauer <i>et al.</i> 2019	M
t_{sh_s}	Bendix A., 2020; Zhou <i>et al.</i> , 2020	M
$t_{sc_{sh}}$	Zhou <i>et al.</i> , 2020	M
$t_{d_{sc}}$	Zhou <i>et al.</i> , 2020	M
$t_{d_{nc}}$	Estimated as one day	M
$t_{r_{ps}}$	Estimated by analogy	L
t_{r_s}	Estimated by analogy	L
$t_{r_{sh}}$	Zhou <i>et al.</i> , 2020	M
$t_{r_{sc}}$	Zhou <i>et al.</i> , 2020	M

Appendix III. Behavioural and intervention parameters per age group: COVID19 case study

Table A3. Behavioural and intervention parameter values per age as selected for the case study

Parameter*	0s	10s	20s	30s	40s	50s	60s	70s	80+
ni_h	10	10	10	10	10	10	10	10	10
$r_{fi_{ps}}$	0.1	0.25	0.5	0.5	0.5	0.5	0.5	0.5	0.5
r_{fi_s}	0.1	0.25	0.5	0.5	0.5	0.5	0.5	0.5	0.5
lpa_h	0.1	0.5	0.75	0.75	0.75	0.75	0.75	0.75	0.75
lpa_{ps}	1	1	1	1	1	1	1	1	1
lpa_s	0.5	0.5	0.5	0.5	0.5	0.5	0.5	0.5	0.5

*Rationale: No reduction factor ($r_{fi_{ps}} = 1$) of their social interactivity respect to healthy ones is applied for pre-symptomatic infected individuals as they are ignorant of their condition; Symptomatic infected individuals are expected to reduce their social interactivity respect to healthy ones as they feel sick ($r_{fi_{ps}} < 1$); The default level of personal protection and awareness (lpa) in children and youngsters is taken as smaller than that of adults; Adult symptomatic individuals are expected to take higher level of personal protection and awareness (lpa_s) to not spread any general disease to others irrespective of the knowledge of their specific condition.

Appendix IV. Default scenarios used for COVID19 outbreak under no interventions

The model simulation of the outbreak time course under the default parameters and no intervention is presented in Figure A4.

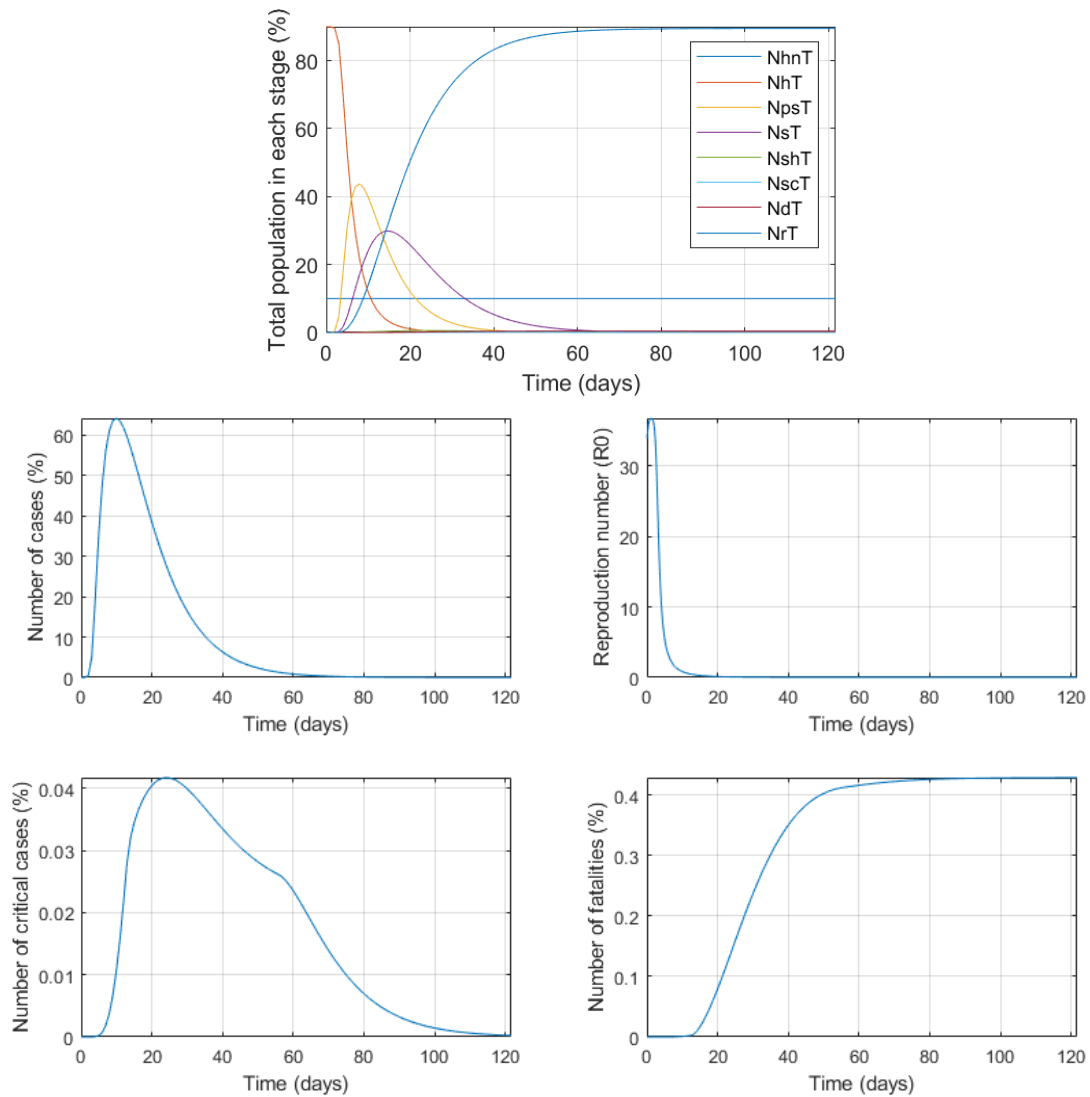


Figure A4. Model simulation of the COVID19 outbreak under no interventions using the default parameters in S1 and S3. The time course profiles of population in each stage is presented (top) as well as those for the total number active cases (middle left); reproduction number (R_0) (middle right); the number of critical cases (bottom left) and the number of fatalities (bottom right). Numbers are in percentage of the total population of all ages.

Appendix V. Matrix of state transitions

Rates Stages	ri_ps (#infPS/d)	ri_s (#infS/d)	rs_ps (#PS-S/d)	rsh_s (#S-SH/d)	rsc_sh (#SH-SC/d)	rd_sc (#SC-D/d)	rr_ps (#PS-R/d)	rr_s (#S-R/d)	rr_sh (#SH-R/d)	rr_sc (#SC-R/d)
N_{nh}	0	0	0	0	0	0	0	0	0	0
N_h	-1	-1	0	0	0	0	0	0	0	0
N_{ps}	1	1	-1	0	0	0	-1	0	0	0
N_s	0	0	1	-1	0	0	0	-1	0	0
N_{sh}	0	0	0	1	-1	0	0	0	-1	0
N_{sc}	0	0	0	0	1	-1	0	0	0	-1
N_d	0	0	0	0	0	1	0	0	0	0
N_r	0	0	0	0	0	0	1	1	1	1

Figure A5. Matrix of state transitions as governed by the infection and transition rates defined.